

**EXPLANATORY
NOTES**



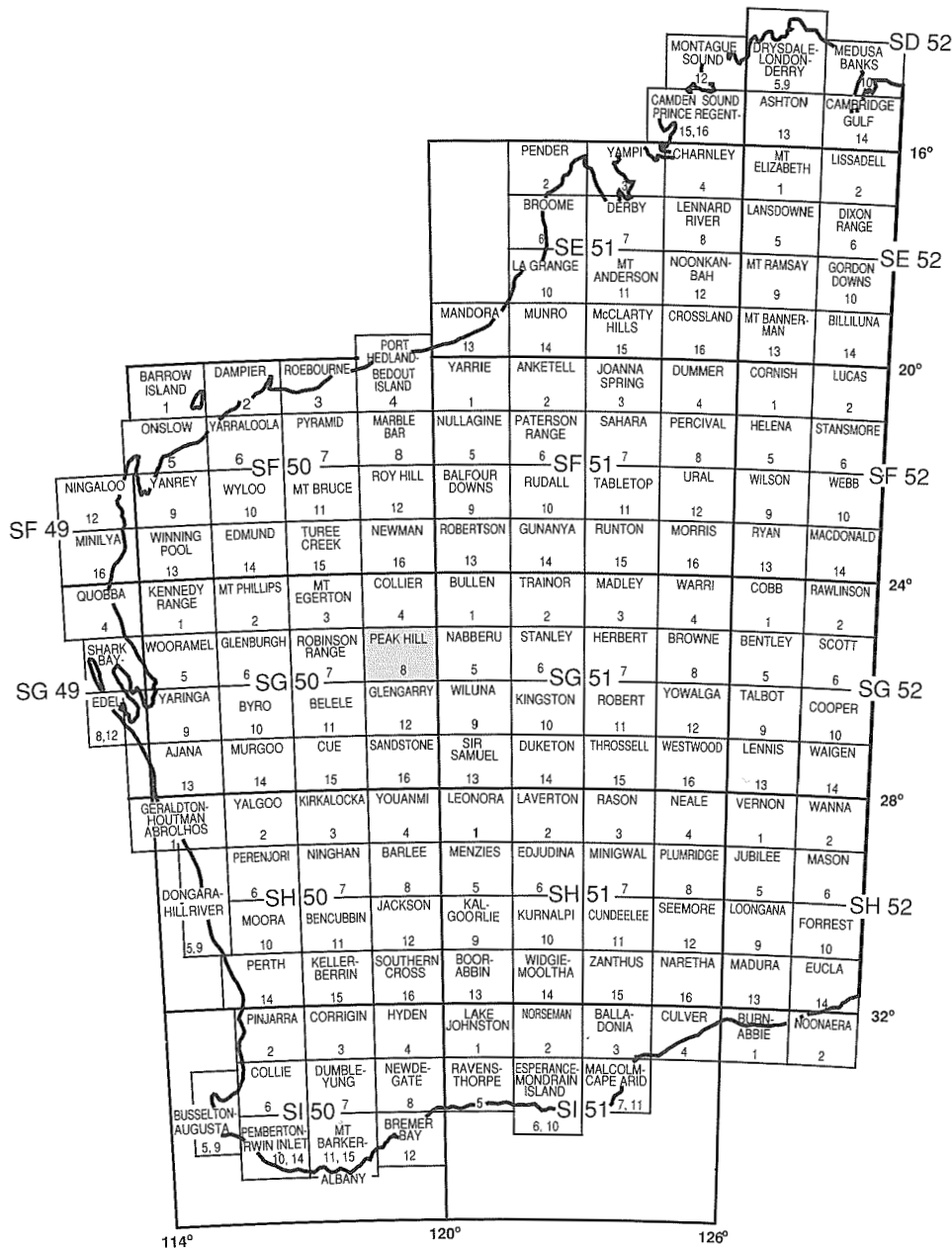
GEOLOGY OF THE BRYAH 1:100 000 SHEET

by F. Pirajno and S. A. Occhipinti

1:100 000 GEOLOGICAL SERIES



**GEOLOGICAL SURVEY OF WESTERN AUSTRALIA
DEPARTMENT OF MINERALS AND ENERGY**



JAMINDI 2647	THREE RIVERS 2747	MARYMIA 2847
PEAK HILL SG50-08		
BRYAH 2646	DOOLGUNNA 2746	THADUNA 2846



GEOLOGICAL SURVEY OF WESTERN AUSTRALIA

**GEOLOGY
OF THE BRYAH
1:100 000 SHEET**

by
F. Pirajno and S. A. Occhipinti

Perth 1998

MINISTER FOR MINES
The Hon. Norman Moore, MLC

DIRECTOR GENERAL
L. C. Ranford

ACTING DIRECTOR, GEOLOGICAL SURVEY OF WESTERN AUSTRALIA
David Blight

Copy editor: K. A. Blundell

The recommended reference for this publication is:

PIRAJNO, F., and OCCHIPINTI, S.A., 1998, Geology of the Bryah 1:100 000 sheet: Western Australia Geological Survey, 1:100 000 Geological Series Explanatory Notes, 41p.

National Library of Australia Card Number and ISBN 0 7309 6581 3

ISSN 1321-229X

Cover photograph:

Outcrops of Narracoota Formation approximately 4 km west of Deadhorse Well, on the BRYAH 1:100 000 map sheet. Mafic schist is in the foreground and a metadolerite sill in the background.

Contents

Access and physiography	3
Geological setting	3
Geochronology	3
Archaean geology	4
Marymia Inlier	4
Granitoid (<i>Agf</i> , <i>Agc</i>) and greenstone rocks (<i>Aci</i> , <i>Aba</i>)	5
Peak Hill Schist (<i>Æp</i> , <i>Æps</i> , <i>Æpc</i> , <i>Æpb</i>)	5
Proterozoic geology	6
Yerrida Group	6
Johnson Cairn Formation (<i>EYc</i>)	6
Doolgunna Formation (<i>EYd</i> , <i>EYdm</i>)	6
Bryah Group	9
Karlundi Formation (<i>EAk</i>)	9
Naracoota Formation (<i>EAn</i> , <i>EAnk</i> , <i>EAnc</i> , <i>EAng</i>)	9
Actinolite schist and chlorite schist (<i>EAns</i>)	10
Metabasite (<i>EAna</i>)	11
Metadolerite dykes (<i>EAnd</i>)	11
Metabasaltic hyaloclastite (<i>EAnh</i>)	11
Metabasaltic vent breccia (<i>EAnx</i>)	12
Jasperoidal chert (<i>EAnc</i>)	13
Ravelstone Formation (<i>EAr</i>)	13
Horseshoe Formation (<i>EAh</i>)	14
Padbury Group	14
Labouchere Formation (<i>EPl</i> , <i>EPli</i> , <i>EPla</i>)	15
Wilthorpe Formation	15
Heines Member (<i>EPwh</i>)	15
Robinson Range Formation (<i>EPr</i> , <i>EPrq</i> , <i>EPri</i>)	15
Millidie Creek Formation (<i>EPm</i>)	16
Earaheedy Group	16
Mount Leake Formation (<i>EEl</i> , <i>EElc</i>)	16
Bangemall Group (<i>EMy</i> , <i>EMw</i> , <i>EMb</i> , <i>EMd</i>)	16
Dolerite dyke (<i>Ed</i>)	16
Structure and metamorphism	19
Structure	19
D ₁ structures	19
D ₂ structures	20
D ₃ structures	21
Discussion and interpretation	21
Metamorphism	21
Ocean-floor metamorphism of metabasaltic hyaloclastite rocks	21
Regional prograde and retrograde metamorphism	22
Volcanic geochemistry	23
Major and trace elements	23
Rare-earth elements	25
Discussion and interpretation	27
Cainozoic geology	27
Mineralization	28
Gold deposits	28
Peak Hill, Jubilee, and Mount Pleasant deposits	28
Harmony deposit	34
Durack prospect	34
Wembley deposit	35
Hit or Miss (Wilgeena) deposit	35
St Crispin prospect	36
Heines Find prospect	36
Goodin Find prospect	36
Ruby Well Group	36
Cashman deposit	36
Mikhaburra deposit	36
Manganese deposits	36
Discussion and interpreted ore genesis for the gold lode mineralization	37
Aeromagnetic and gravity data	37
Acknowledgements	39
References	40

Figures

1. Simplified geology of the Bryah, Padbury, and Yerrida Basins	2
2. Photomicrograph showing a porphyroblast in quartz–muscovite schist	5
3. Outcrop of quartz mylonite	7
4. Photomicrograph illustrating the S–C planes of the Peak Hill Schist mylonite	7
5. Photomicrograph of mylonitic quartz–biotite(–albite) schist from the Mine sequence	8
6. Photomicrograph of mylonite from the Hangingwall sequence	8
7. Typical outcrop of Narracoota Formation mafic schist	10
8. Photomicrograph showing pyroclastic texture in Narracoota Formation mafic schist	11
9. Photomicrograph of basaltic hyaloclastite	12
10. Volcanic breccia intersected in diamond drillhole BD1	13
11. Schematic stratigraphic column of the Horseshoe Formation	14
12. Examples of millimetre-scale microbands in the BIF of the Robinson Range Formation	16
13. Simplified geology of the Padbury and Bryah Basins	19
14. Sketch illustrating the possible formation of D_1 structures and F_1 folds and faults	20
15. Triangular plot of $(Na_2O + K_2O) - FeO_{total} - MgO$ for the Narracoota Formation volcanic rocks	24
16. Total-alkali versus silica plot for the Narracoota Formation volcanic rocks	24
17. Cr versus Cu/Ni diagram for metabasites of the Narracoota Formation	24
18. Jensen (1976) cationic plot of Narracoota Formation rocks	24
19. Tectonic discriminant diagram for the Narracoota Formation volcanic rocks	26
20. TiO_2 versus FeO/MgO diagram for the Narracoota Formation volcanic rocks	26
21. Chondrite-normalized REE abundances of Narracoota Formation volcanic rocks	26
22. Model of a possible palaeoenvironmental setting of the Narracoota Formation	27
23. Distribution of mineral deposits and position of Bouguer gravity anomalies	29
24. Simplified geological map of the Fiveways, Main, and Mini pits	31
25. Peak Hill Mini pit mylonitic schist, graphitic schist, and Marker quartzite	32
26. Albite porphyroblasts in mylonitic schist at Mount Pleasant	32
27. Photomicrograph of the Mine sequence schist	33
28. Photomicrograph of the Hangingwall sequence graphitic mylonite schist	34
29. Diagrammatic cross section of the Harmony ore zones	35
30. Aeromagnetic image of BRYAH	38
31. Gravity model of a north–south section across Narracoota Formation rocks	39

Tables

1. Stratigraphy of the Yerrida, Bryah, and Padbury Basins	4
2. Relationship between diagnostic metamorphic minerals and deformation	17
3. Prograde metamorphic assemblages of the Bryah Group and possible precursor rocks	22
4. Metamorphic assemblages of the Peak Hill Schist and possible precursor rocks	22
5. Averages of major- and trace-element analyses of the Narracoota Formation	23
6. Rare-earth element representative analyses of the Narracoota Formation	25
7. Gold production prior to December 1995 from mines, prospects, and deposits on BRYAH	30
8. Copper and manganese production prior to December 1995 on BRYAH	36

Geology of the Bryah 1:100 000 sheet

by

F. Pirajno and S. A. Occhipinti

The BRYAH¹ 1:100 000 map sheet (SG50-08-2646) covers an area bounded by latitudes 25°30'S and 26°00'S and longitudes 118°30'E and 119°00'E, located in the southwestern part of the PEAK HILL 1:250 000 sheet (Fig. 1). The geology of BRYAH has previously been described in Explanatory Notes for early editions of the PEAK HILL 1:250 000 map sheet (MacLeod, 1970; Gee, 1987). The general geology of BRYAH and surrounding areas have also been discussed by Gee (1979), Barnett (1975), and Hynes and Gee (1986).

BRYAH is dominated by rocks belonging to the Glengarry Basin, as originally defined by Gee (1990) and Gee and Grey (1993). These rocks also cover the greater part of PEAK HILL and GLENGARRY (1:250 000), and minor portions of WILUNA (1:250 000) and ROBINSON RANGE.

The Glengarry Basin as defined by Gee (1990) and Gee and Grey (1993) contained the Glengarry and Padbury Groups. Recent detailed geological mapping, integrated with aeromagnetic and Landsat image interpretations, indicates that the Glengarry Basin has a more complex tectonic architecture and depositional history than originally thought. In this recent work, Pirajno et al. (1996) found that the previously defined Glengarry Basin can be assigned to three distinct groups: the Bryah and Padbury Groups in the west, and the Yerrida Group in the east and southeast (Fig. 1). The rocks of the Bryah, Padbury, and Yerrida Groups have distinctive stratigraphic, structural, and metamorphic characteristics. The contacts between the Bryah and Padbury Groups are generally tectonic (Occhipinti et al., 1996), although some depositional (unconformable) contacts have also been reported (Martin, 1994; Occhipinti et al., 1996). The boundary between the Bryah and Yerrida Groups is tectonic and marked by the northeast-trending Goodin Fault (Fig. 1).

Pirajno et al. (1996) and Pirajno (1996) also suggested that the Bryah and Yerrida Groups were deposited in separate depocentres, named the Bryah and Yerrida Basins respectively. Thus the names Glengarry Group and Glengarry Basin should be abandoned. In addition, Martin

(1994) and subsequent workers (Occhipinti et al., 1996; Pirajno et al., 1996) considered the Padbury Group to have been deposited in a peripheral foreland basin (Padbury Basin) on top of the Bryah Group. Tectonic evolution models of the Bryah and Yerrida Basins are discussed in Pirajno et al. (1995a) and Pirajno (1996).

The area covered by BRYAH is of particular importance, as it contains significant precious metal deposits and a large area of mafic and ultramafic rocks. These rocks belong to the Narracoota Formation, and represent a key component in the understanding of the tectonic evolution of the Bryah Basin.

The Peak Hill deposit, and the recently discovered Harmony deposit, are major producers in the Murchison Field District with resources in excess of 20 t of gold (see Table 7, page 30). The Peak Hill deposit is contained within the Peak Hill Schist, whereas the Harmony deposit is in the regolith and rocks of the Bryah Group. Other past and present producers in the Murchison Field District are the Fortnum and Labouchere gold deposits, which lie to the northwest of the Peak Hill and Harmony mines, on ROBINSON RANGE. Accounts of the early history and discovery of gold in the Peak Hill area are provided by Heydon (1991) and de Havilland (1985, 1986).

BRYAH covers the eastern part of the Bryah Basin, the southwestern part of the Marymia Inlier, the Peak Hill Schist, the western part of the Yerrida Basin, and the eastern parts of the Padbury Basin. Also included are the southernmost edge of the Bangemall Basin and some small outliers of the Earraheedy Group (Fig. 1).

In these Notes, coordinates are expressed in terms of the Australian Map Grid (AMG — Zone 50 J) standard six-figure reference system whereby the first group of three figures (eastings) and the second group (northings) together uniquely define position, on this sheet, to within 100 m. The prefix 'meta' is used to denote metamorphosed rocks in which the preservation of the original textures allows the recognition of the precursor rock type with a good degree of confidence (e.g. metabasalt). The term 'metabasite' is used for rocks of obvious basic composition, but for which metamorphism or alteration has largely obliterated the original textures of the precursor rock (e.g. basalt, dolerite, or pyroxenite).

¹ Capitalized names refer to 1:100 000 and 1:250 000 map sheets.

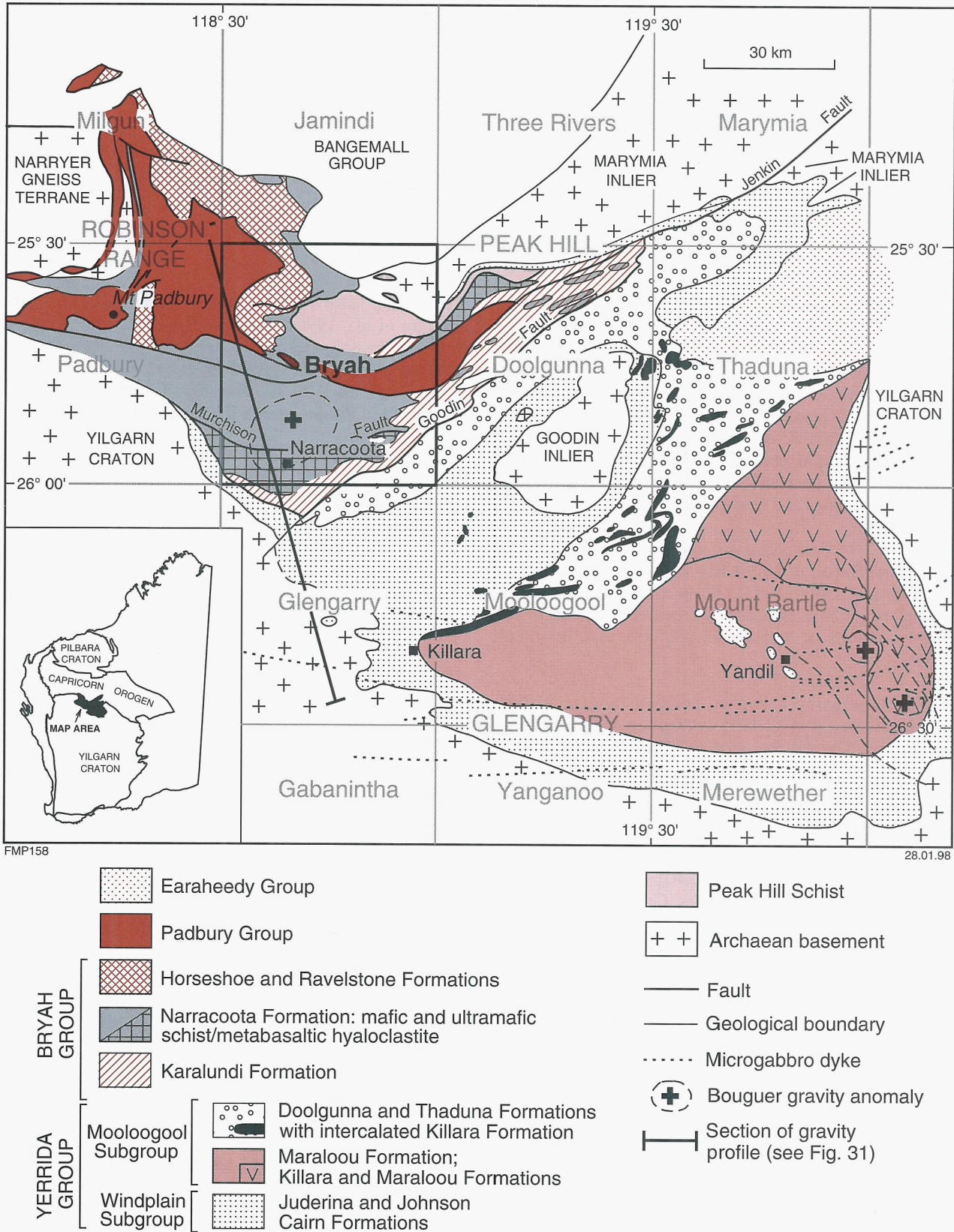


Figure 1. Simplified geology of the Bryah, Padbury, and Yerrida basins, modified from Pirajno et al. (1996), and location of the BRYAH 1:100 000 map sheet

Access and physiography

The sealed Great Northern Highway runs through the southeastern part of BRYAH in an east-northeast direction. The unsealed Ashburton Downs – Meekatharra road extends north from the Great Northern Highway and provides access to the Harmony, Peak Hill, Fortnum, Labouchere, Horseshoe, and Horseshoe Lights mines.

Meekatharra is the nearest town. It lies 72 km to the south, from the point where the Great Northern Highway crosses the southern boundary of BRYAH. Apart from the Peak Hill mine, other inhabited centres include the Julga Jinna aboriginal settlement, situated at the foot of the Robinson Range near Fraser Well (northwestern part of BRYAH); and the Narracoota and Bryah pastoral homesteads, in the south and at the northern boundary respectively.

The Murchison River, which flows westward through the southern portion of BRYAH, is the main drainage system in the area. On BRYAH, two major tributaries of the Murchison River flow southward in broad valleys cutting through the hills of the Robinson Range. The northern divide of the Murchison River drainage system forms an arcuate line. This divide trends east along the Peak Hill Schist mylonites and northwest along ridges of the Labouchere Formation. North of this divide, the drainage flows into the westerly flowing Gascoyne River about 35–40 km to the north.

The physiography of BRYAH reflects the geology. The most prominent physiographic feature is the Robinson Range, which forms lines of hills largely made up of banded and granular iron-formation. In contrast the valleys separating the hills are underlain by softer shales. The Robinson Range reaches altitudes of up to 657 m above sea level, although the relief is a little over 100 m above the surrounding countryside. The remaining areas on BRYAH are essentially flat or with gently rolling hills formed by the weathering of mafic metavolcanic and metasedimentary rocks.

Geological setting

The Palaeoproterozoic Padbury, Bryah, and Yerrida Basins lie in the southern part of the Capricorn Orogen — a major zone of deformed, low- to high-grade metamorphic rocks and granitoid intrusions that developed during continental collision between the Pilbara and Yilgarn Cratons about 2000–1800 Ma (Tyler and Thorne, 1990; Myers, 1993; Myers et al., 1996). As mentioned previously, the Glengarry Group — originally defined by Gee and Grey (1993) — has now been redefined to comprise the Bryah and Yerrida Groups (Fig. 1). These two groups are present in both the western and eastern parts of the former Glengarry Basin. They contain different stratigraphic successions and structural histories, and are everywhere in faulted contact with each other. Based on these observations, Pirajno et al. (1995a), Pirajno and Occhipinti (1995), and Pirajno et al. (1996) proposed that the Glengarry Basin of Gee and Grey (1993) be considered as two separate basins, namely the

Yerrida and Bryah Basins, containing the Yerrida and Bryah Groups respectively.

The Yerrida Group, in the southern part of BRYAH, is primarily represented by the Doolgunna Formation. The contact between the Doolgunna Formation and the Bryah Group (Karatundi Formation) is along the northeast-trending Goodin Fault — a major structure separating the Bryah and Yerrida basins (Fig. 1).

The Padbury Group is now considered to have been deposited in a third and separate basin — the Padbury Basin — which was developed on top of the Bryah Group (Windh, 1992; Martin, 1994; Martin, in prep.; Occhipinti et al., 1996). A simplified stratigraphy for the Padbury, Bryah, and Yerrida Groups is shown in Table 1.

The tectonic units present on BRYAH are (see simplified geology inset on the geological map):

- the Marymia Inlier in the northeast, consisting of Archaean granite gneiss and minor amounts of greenstone;
- the Peak Hill Schist, in the north-central part, consisting of mylonitized and metamorphosed rocks, derived from a quartz-rich and/or quartzofeldspathic precursor;
- parts of the Palaeoproterozoic Yerrida, Bryah, and Padbury Basins;
- a small portion of the Mesoproterozoic Bangemall Basin in the north; and
- small outliers of the Palaeoproterozoic Earraheedy Group in the south-central parts.

Geochronology

The age of the Marymia Inlier has been investigated by researchers at the University of Western Australia. Zircon dating of two porphyry boudins enclosed in greenstone rocks at the Marymia gold deposit, about 100 km to the northeast of BRYAH, gave ages of 2696.5 ± 7.1 Ma and 2690 ± 13 Ma (McMillan, N., 1995, pers. comm.; McMillan, 1993). Sensitive High-Resolution Ion Microprobe (SHRIMP) U–Pb zircon dating of augen gneiss near the contact with the Peak Hill Schist gave an age of 2672 ± 3 Ma (Nelson, 1996).

The age of the Yerrida Group is constrained by the age (2.65 Ga) of the underlying Yilgarn Craton (Myers, 1990) and the age (2.0–1.8 Ga) of the overlying Earraheedy Group (Grey, 1994; Nelson, 1996). Absolute dating on the Yerrida Group is confined to Pb–Pb isochrons of 2258 ± 180 Ma (Russell et al., 1994) and 2173 ± 64 Ma (Woodhead and Hergt, 1997) on stromatolitic carbonate from the newly defined Bubble Well Member of the Juderina Formation, near the base of the Yerrida Group. Thus, on present evidence, the age of the Yerrida Group is bracketed between 2.25 and 1.8 Ga.

The ages of the Bryah and Padbury Groups are poorly constrained. A Pb–Pb isochron date of 1920 ± 35 Ma, on assumed syngenetic pyrite from the Narracoota

Table 1. Stratigraphy of the Yerrida, Bryah, and Padbury Basins

Basin/Group	Formation/Member	Rock types
PADBURY BASIN (peripheral foreland basin)		
Padbury Group	Millidie Creek	sericitic siltstone, chloritic siltstone, BIF, dolomitic arenite
	Robinson Range	ferruginous shale, BIF
	Wiltorpe	quartz-pebble conglomerate
	Beatty Park Member	mafic siltstone/wacke
	Heines Member	polymictic conglomerate
	Labouchere	turbidite sequence (quartz wacke, siltstone)
~~~~~ Unconformable contact — in places tectonized ~~~~~		
<b>BRYAH BASIN</b> (succession)		
<b>Bryah Group</b>	Horseshoe	BIF, wacke, shale
	Ravelstone	quartz-lithic wacke
	Narracoota	mafic-ultramafic volcanic rocks and dykes, tuffs, and intercalated sedimentary rocks
	Karalundi	conglomerate, quartz wacke
~~~~~ Faulted contact ~~~~~		
YERRIDA BASIN		
Yerrida Group		
	Mooloogool Subgroup (rift succession)	black shale, siltstone, carbonate
	Intercalated	aphyric mafic lavas and intrusives
	Killara	diamictite, arkosic sandstone, siltstone, shale
	Doolgunna	lithic wacke, siltstone, shale, minor arkose
	Thaduna	
Windplain Subgroup (sag-basin succession)	Johnson Cairn	siltstone, shale, carbonate, minor lithic wacke
	Juderina	arenite, conglomerate, minor carbonate
	Bubble Well Member	silicified carbonate with evaporite units
	Finlayson Member	arenite
~~~~~ Unconformity on Yilgarn Craton ~~~~~		

Modified from Pirajno et al. (1996)

Formation (Bryah Group), was reported by Windh (1992). A Pb–Pb age of 1.7 Ga from galena from the Mikhaburra mine (Narracoota Formation — Bryah Group) may represent a mineralizing event (Blockley, J., 1995, pers. comm., and unpublished data). A maximum age of  $2014 \pm 22$  Ma, from U–Pb dating of detrital zircons in the Ravelstone Formation (Bryah Group), was obtained by Nelson (1996). Windh (1992) reported U–Pb detrital zircon ages of 2.0 and 1.9 Ga from the Labouchere Formation of the overlying Padbury Group. More recently, Nelson (1996) determined a maximum depositional age of the Beatty Park Member (Padbury Group), which overlies the Labouchere Formation, at  $1996 \pm 35$  Ma (SHRIMP U–Pb).

On BRYAH, outliers of the Mount Leake Formation (which has been correlated with the Earahedy Group) lie along the valley of the Murchison River and unconformably overlie the Bryah Group. Glauconite obtained from quartz arenite outcrops of the Mount Leake Formation, near Bilyuin, returned a K–Ar age of 1573 Ma (Bunting, 1986). This age, however, is not considered reliable by Grey (1994), who reviewed the geochronological data from the Earahedy Group. Grey (1994) concluded that the only reliable date available at the time is a Rb–Sr age of about 1630 Ma for emplacement of quartz syenite in the Teague Ring Structure, on the southern margin of the Earahedy

Basin, and that the true age of sedimentation was probably older than 1.8 Ga. This interpretation is supported by limited biostratigraphic evidence (Grey, 1994) and by Pb–Pb dating of stromatolitic carbonate from the Yelma Formation, which gave ages of  $2008 \pm 68$  Ma and  $1946 \pm 71$  Ma (Russell et al., 1994). A minimum depositional age of  $1785 \pm 11$  Ma is deduced from recent U–Pb dating of detrital zircons (samples collected from the glauconitic arenite in the Bilyuin area; Nelson, 1996).

The Bangemall Basin lies in the northern part of BRYAH and includes the Backdoor Formation, which is unconformable on the Bryah Group. The age of the Bangemall Group elsewhere is constrained by a Pb–model age of 1.64 Ga from the Abra deposit and a U–Pb age of 1.63 Ga from the Tangadee Rhyolite (Nelson, 1995).

## Archaean geology

### Marymia Inlier

The Marymia Inlier (Windh, 1992; Marymia Dome of Gee, 1987) represents a fragment of Archaean granite–greenstone basement. The inlier trends northeast and its



tectonized southwestern tip is exposed in the northeastern part of BRYAH (Fig. 1).

### Granitoid (*Agf*, *Agc*) and greenstone rocks (*Aci*, *Aba*)

On BRYAH, rocks of the Marymia Inlier are mainly granitic (*Agf* and *Agc*), but also include small enclaves of calc-silicate rock, orthoamphibolite (*Aba*), and minor amounts of metamorphosed banded iron-formation (BIF — *Aci*). The Peak Hill Schist (*Ap*) is also tentatively placed within the Marymia Inlier. The granitic rocks are locally strongly foliated to gneissic or display strong cataclastic fabrics. Granitic rocks include both fine-grained (aplitic) and coarse-grained porphyritic phases. Some outcrops previously mapped as granite by Gee (1987) have been included in the Peak Hill Schist, as they lack unequivocal granitic textures and are similar to other units of the Peak Hill Schist succession (see below).

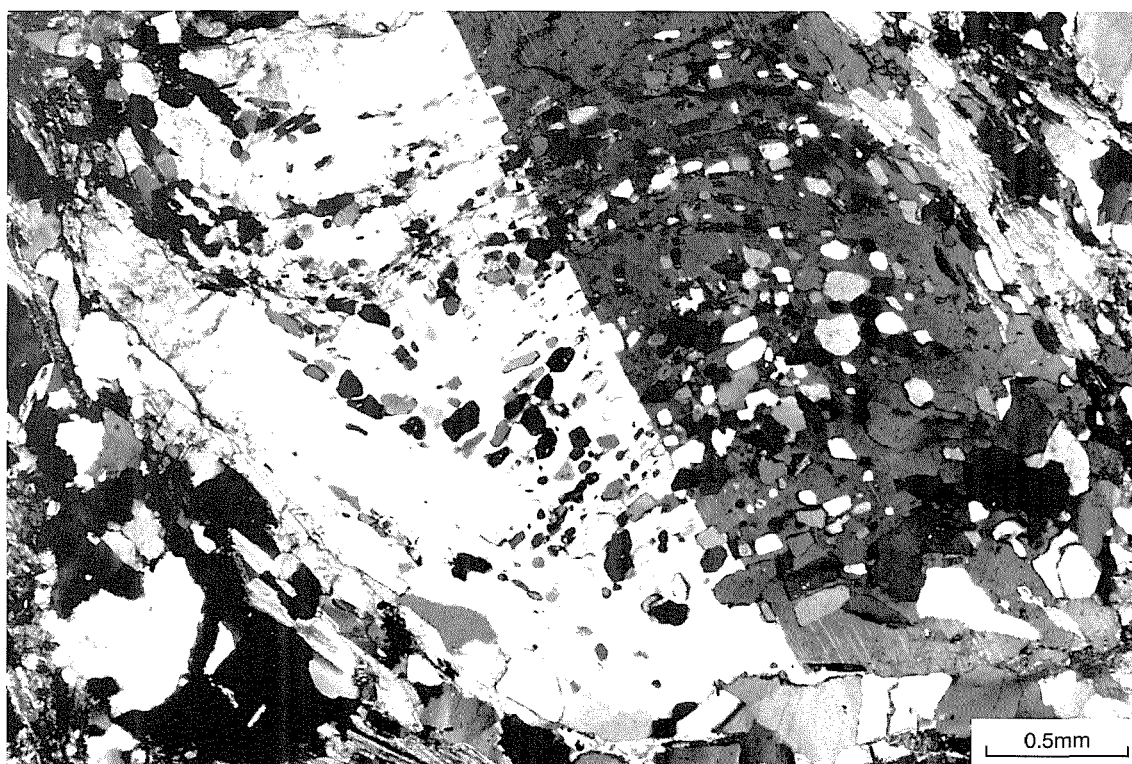
The contact between the mainly granitic rocks of the Marymia Inlier and the Peak Hill Schist is poorly exposed, although field observations suggest that this contact may be tectonically interleaved. Close to the contact, the granite of the Marymia Inlier becomes more deformed and is characterized by gneissic banding. Outcrops of augen gneiss containing large (up to 2 cm in diameter) K-feldspar porphyroblasts lie about 4 km east-southeast of the Old Peak Hill Homestead. Outside

BRYAH, to the east, the Marymia granitic rocks are monzogranite, which show increasing cataclastic deformation towards the southwest.

### Peak Hill Schist (*Ap*, *Aprs*, *Aprc*, *Aprb*)

The Peak Hill Schist forms a tectonic unit of uncertain age that covers an elliptical area in the northern part of BRYAH. The area covered by this unit was formerly subdivided into the Peak Hill Metamorphic Suite, the Doolgunna Formation, and the Crispin conglomerate (Gee, 1987), and also included part of the Marymia Dome of Gee (1987). The Peak Hill Schist appears to be continuous with the Marymia Inlier. Thornett (1995) suggested that the 'Peak Hill Dome' represents the deformed southwestern end of the Marymia Inlier and based this view on aeromagnetic data. Field observations, integrated with Landsat and aeromagnetic image interpretations support this; although, given that the absolute age of the Peak Hill Schist is unknown, it has not been formally assigned to the Archaean.

The intensity of deformation and Proterozoic regional metamorphism decreases towards the northeast and the Marymia Inlier, where the granitoid rocks are undeformed. The boundary between the Peak Hill Schist and the Marymia Inlier is a zone of intense deformation and recrystallization. This boundary is not well defined (Gee, 1987), but is a complex zone of tectonic inter-



FMP 170

20.11.97

Figure 2. Photomicrograph showing a rotated alkali feldspar porphyroblast in quartz-muscovite schist (Peak Hill Schist). GSWA 136781, crossed polars

leaving. In addition, areas previously identified as porphyritic granite of the Marymia Inlier are in fact quartz–muscovite–biotite(–chlorite) schist with rotated alkali feldspar porphyroblasts of the Peak Hill Schist (Fig. 2).

Rocks of the Peak Hill Schist include phyllonite, quartz–muscovite schist, quartz–muscovite–biotite schist, calc-silicate, sericite schist, and quartz–muscovite–biotite(–chlorite) schist with alkali feldspar porphyroblasts and minor amounts of metabasite. These units have been variously deformed to form a range of mylonitic textures. The Peak Hill mylonite (*Apb*) and Crispin mylonite (*Apc*) are also included in the Peak Hill Schist. These units form arcuate zones, and have been interpreted as representing former fault planes (possibly thrusts) and, therefore, high-strain zones. In the area of the Peak Hill and Jubilee gold deposits, relatively undeformed metadolerites (possibly sills) are present, but it is not certain whether these are part of the Peak Hill Schist or whether they are a tectonic fragment of the Narracoota Formation.

The Peak Hill Schist was subjected to three deformation events and two periods of low- to mid-grade greenschist facies metamorphism. Isolated amphibolite facies assemblages from drillcore within this unit have been reported by Thornett (1995).

The Peak Hill Schist can be separated into units dominated by quartz–muscovite schist (*Ap*) and units dominated by sericite schist (*ApS*). The latter consists mainly of sericite with minor amounts of quartz, whereas most of the former contains abundant quartz. This difference may be a reflection of the precursor lithologies, and it is possible that the sericite schist may have been largely derived from either arkosic or granitic material, whilst the quartz-rich schist may have been derived from more quartz-rich sedimentary rocks. Another unit of the Peak Hill Schist is a quartz–magnetite–spessartine mylonite. Only one outcrop of this rock was observed on BRYAH. The abundant spessartine and magnetite suggest that its precursor may have been an iron–manganese-rich chemical sediment or exhalite (Stanton, 1989).

The Peak Hill mylonite (*Apb*; Fig. 3) and the Crispin mylonite (*Apc*) are tectonic units within the Peak Hill Schist. The Peak Hill mylonite (*Apb*) is important because it is spatially associated with the Peak Hill – Mount Pleasant gold mineralization. This unit shows up well on Landsat imagery, with a light-greenish grey spectral response (bands 4, 1, and 7). It is a distinct quartz blastomylonite (Passchier and Trouw, 1966) and quartz mylonite lens that has been refolded within the quartz muscovite schist. Other, and less conspicuous, quartz blastomylonite and quartz mylonite lenses are common within the Peak Hill Schist, where they have been previously mapped as chert or banded chert (e.g. Windh, 1992). The mylonitic fabric of these rocks is revealed under the microscope, where S–C surfaces are clearly distinguishable by lines of mica ‘fish’¹ (Lister and Snoke,

1984) in a dominantly and variably recrystallized quartz matrix (Figs 4–6; and also see **Structure**). In some cases pervasive dynamic recrystallization resulted in the obliteration of the original mylonitic fabric. The blastomylonites are interpreted as linear structures that developed along faults (possibly thrust planes), where there was repeated shear movement during deformation.

The Crispin mylonite (*Apc*) trends northwest and lies in the southern part of the Peak Hill Schist outcrop area, between the sericite schist and the dominantly quartz–muscovite schist. This unit has an elongate lenticular shape and extends from a point about 5 km south of the Peak Hill village, eastward, to the vicinity of the old Hit or Miss mine. The Crispin mylonite, which was referred to by Gee (1987) as the Crispin conglomerate, is characterized by square to rounded quartz arenite clasts (up to 60 cm in length) in a sericite-rich matrix. The conclusion that this unit is not a conglomerate, but a mylonite, is based on mesoscopic and microscopic observations, which indicate that both matrix and clasts display mylonitic fabrics. Mylonites that look like conglomerates (pseudo- or tectonic conglomerates) have also been reported by Peters (1993) and Raymond (1984a,b).

## Proterozoic geology

### Yerrida Group

The Yerrida Group was deposited in the Yerrida Basin and contains two subgroups that were deposited in two sub-basins: Windplain and Mooloogool. The Windplain Subgroup contains the basal units of the Yerrida Group, and was accumulated in a sag basin within an epicontinental environment (Pirajno et al., 1996). Small outcrops of the Johnson Cairn Formation, belonging to this subgroup, are present in the southwestern part of BRYAH. The Mooloogool subgroup is a northeast-trending succession of clastic sedimentary and mafic igneous rocks (Pirajno et al., 1996). This subgroup is present in the southeastern part of BRYAH, and is represented only by the dominantly clastic rocks of the Doolgunna Formation.

### Johnson Cairn Formation (*EYc*)

On BRYAH the Johnson Cairn Formation (*EYc*) consists of ferruginous shale and is only observed in a small outcrop around Cheroona Well.

### Doolgunna Formation (*EYd*, *EYdm*)

The Doolgunna Formation (*EYd*) is isoclinally folded and consists of moderately sorted arkose and quartz wacke, with interbedded conglomerate. Diamictite² units (*EYdm*) are present south of the Great Northern Highway, near

¹ Mica fish: During the process of mylonitization, mica laminae become reduced in size and with ongoing recrystallization the micas are further reduced in size, so that the mylonite fabric is defined by thin relict micas, commonly linked by thin trails, which separate quartz-rich areas (Lister and Snoke, 1984).

² Diamictite is a non-genetic term applied to non-sorted, generally terrigenous sediment containing a wide range of clasts and particle sources that are set in a muddy matrix (Bates and Jackson, 1987). The term ‘diamictite’ is commonly used for a deposit of glacial origin, however this interpretation is incorrect and in such cases the unit is in fact a tillite. In the Doolgunna Formation the diamictite consists of small to very large (centimetres to tens of metres) exotic blocks contained in a shaly (locally sericitic) matrix.



FMP 172

18.11.97

**Figure 3. Outcrop of quartz mylonite (Peak Hill Schist). Note the flaggy nature of this rock and its steep dip**

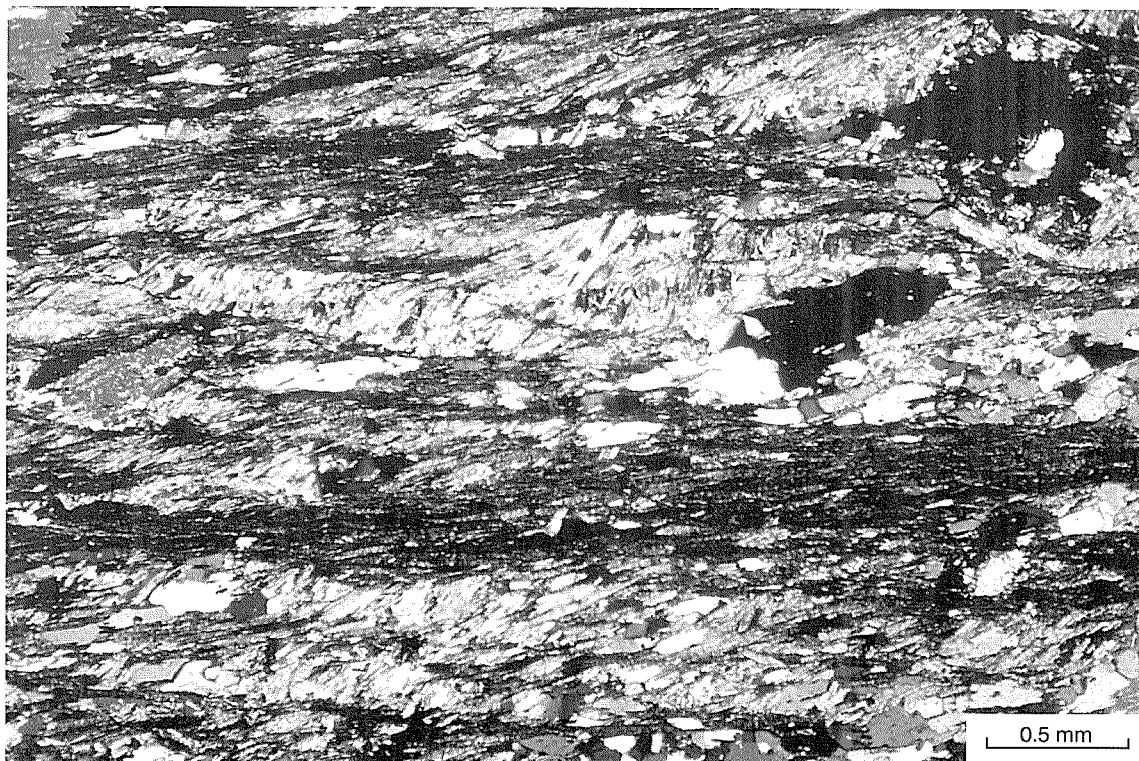


**Figure 4. Photomicrograph from the Peak Hill Schist mylonite, illustrating a typically mylonitic fabric and S-C planes (C planes are horizontal, S planes trend from upper right to lower left between the C planes). Also note the mica fish on the left of the photomicrograph. GSWA 120826, crossed polars**



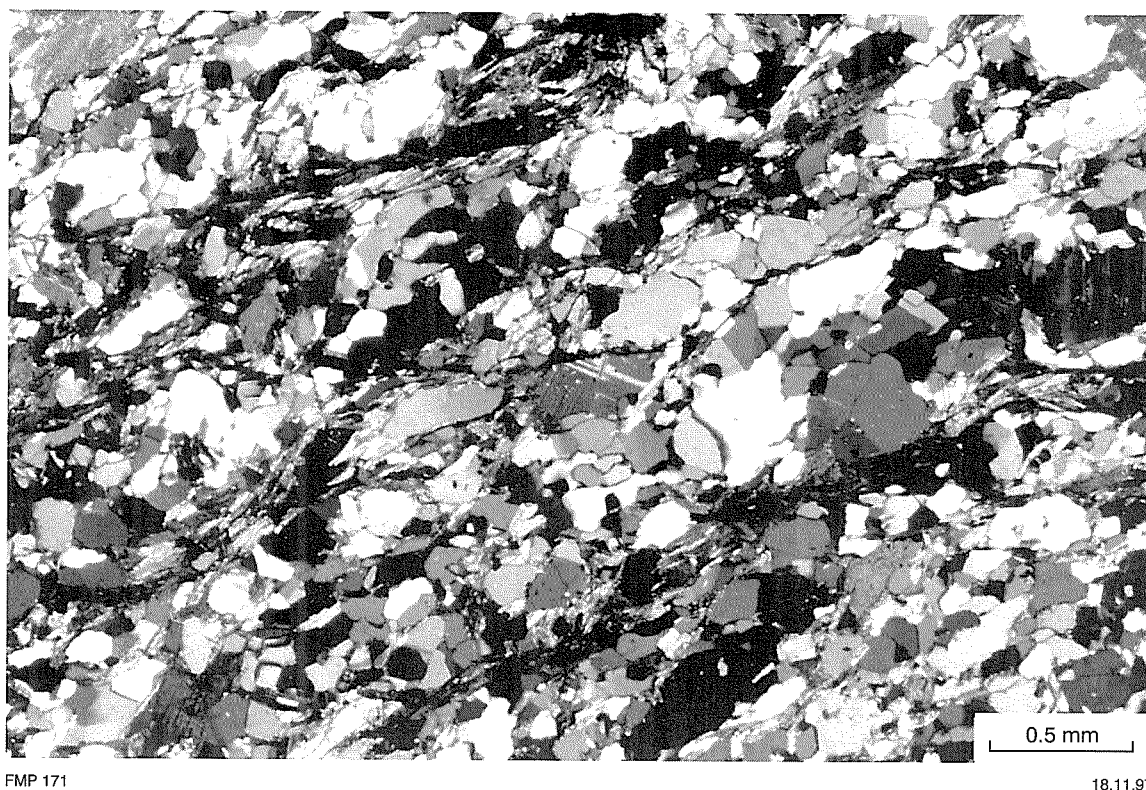


Figure 5. Photomicrograph from the Peak Hill Schist mylonite, illustrating a partially recrystallized fabric. This sample is a mylonitic quartz–biotite(–albite) schist from the Mine sequence in which biotite defines C planes. The S planes are no longer visible due to recrystallization to a blastomylonite. GSWA 119792, crossed polars

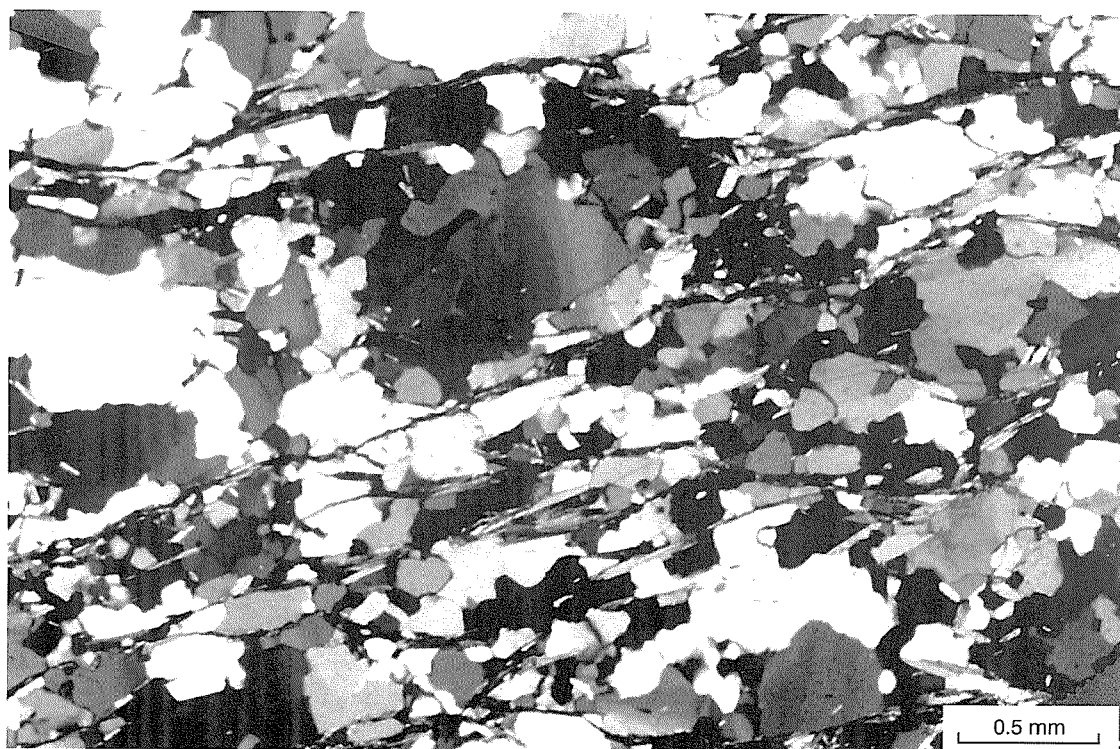


Figure 6. Photomicrograph from the Peak Hill Schist mylonite of the Hangingwall sequence. The C surfaces have survived recrystallization and now form thin mica trails. GSWA 119723, crossed polars



Goodin Find, and about 7 km to the northeast near White Well. This diamictite is probably the result of mass wasting, sourced from the Goodin Inlier, that accumulated in a northeast-trending graben structure — one side of which was formed by the uplifted Inlier (Pirajno, 1996). On the adjacent DOOLGUNNA to the east (Adamides, 1995) the diamictites contain angular blocks several tens of metres in length.

The total thickness of the Doolgunna Formation is not known, but taking into consideration the folding, an estimate of 3000 m is considered possible. Sedimentary structures are locally well developed and include graded bedding, flame structures, and cross-bedding. In the area 6 km southeast of Don Bore, rip-up clasts and scour marks are indicative of a high-energy environment.

## Bryah Group

The Bryah Group was deposited in the Bryah Basin, and consists of deformed and metamorphosed mafic–ultramafic volcanic, clastic, and chemical sedimentary rocks.

The Bryah Group is subdivided (older to younger) into the Karalundi, Narracoota, Ravelstone, and Horseshoe Formations. The Karalundi Formation includes an immature to moderately mature clastic succession of rift fill facies, and conformably underlies the Narracoota Formation. The Narracoota Formation is the volcanic component of the Bryah Basin. It includes dominantly metabasaltic rocks, which occupy most of the southern half of BRYAH and extend northward — to the west and north of the Peak Hill Schist. The geochemistry of the mafic igneous rocks of the Narracoota Formation, which is discussed later in **Volcanic geochemistry**, indicates that the rocks have an oceanic affinity. It is also important to note that the distribution of the Narracoota Formation in the southern part of BRYAH coincides with a positive gravity anomaly (Fig. 23, page 29).

The Narracoota Formation is disconformably overlain by the Ravelstone Formation — a turbidite facies clastic unit. Interfingering between the lower part of the Ravelstone Formation and the Narracoota Formation may be due to shearing along the contact. The Ravelstone Formation grades upward into the Horseshoe Formation, which includes clastic, argillaceous, and chemical sedimentary rocks (BIF). The Horseshoe Formation is overlain by the dominantly clastic quartz-rich rocks of the Labouchere Formation (Padbury Group), which hosts important mesothermal lode gold deposits to the northwest on MILGUN (Swager and Myers, 1997).

The Bryah Group is overlain by the Padbury and Bangemall Groups, and by the Mount Leake Formation. The contacts with the Padbury Group commonly appear to be faulted, or conformable (Occhipinti et al., 1996), but also have been reported to be unconformable by Martin (1994). The Bangemall Group and the Mount Leake Formation unconformably overlie rocks of the Bryah Group. The Bryah Group's lower boundary, where exposed, is faulted; either against Archaean granite, the Peak Hill Schist, or the Yerrida Group.

## Karalundi Formation (*PAk*)

On BRYAH the Karalundi Formation (*PAk*) outcrops 3.5 km east of Wilgeena mine and in the southeast (along the Great Northern Highway, in the Don Bore and Goodin Find areas) where Karalundi lithologies are in faulted contact with the Doolgunna Formation. The Karalundi Formation includes chert; siltstone; calcareous siltstone; cross-bedded arenite and ferruginous arenite; litharenite; purple, green, and black shale; and minor quartz-pebble conglomerate lenses.

In areas immediately south of the southern sheet boundary of BRYAH, in the northwestern part of GLENGARRY (Pirajno et al., 1997), the Karalundi Formation intercalates with basaltic volcanoclastic rocks of the Narracoota Formation. The Karalundi Formation also contains pods of hematitic jasperoidal chert, which have been interpreted by Gee (1979, 1987) as fumarolic pipes.

## Narracoota Formation (*PAn*, *PAnk*, *PAnc*, *PAnq*)

The Narracoota Formation is a new name (Occhipinti et al., 1997a) and it includes most of the Narracoota Volcanics — as defined by Gee (1987, 1990) and Gee and Grey (1993) — and minor amounts of intercalated sedimentary rocks (*PAnq*).

Rocks of this formation occupy most of the south-central part of BRYAH. In the northern part of BRYAH the Narracoota Formation surrounds, and is in tectonic contact with, the Peak Hill Schist to the south, west, and northwest. The Narracoota Formation conformably overlies and locally interfingers with the Karalundi Formation, and also interfingers, and/or is in disconformable contact, with the base of the Ravelstone Formation. Contacts between the Narracoota Formation and the Padbury Group are tectonic. In the north, regional structural relations suggest that the Narracoota Formation is also in tectonic contact with the Horseshoe Formation. South of the Robinson Range, small lenses of sedimentary rock (lithic wacke and shale — *PAnq*) are intercalated with the volcanics of the Narracoota Formation.

On BRYAH the Narracoota Formation can be subdivided — based on texture, geochemistry, and petrology — into mafic schist, ultramafic schist, and basaltic hyaloclastite. The first two are characterized by a pervasive schistosity, and the distinction between mafic and ultramafic composition can only be ascertained geochemically (see below). The mafic–ultramafic schist includes actinolite–tremolite schist and chlorite schist. Metadolerite dykes and sills, metabasaltic breccia, and minor metapyroxenite lenses are contained within the schists, and although these rocks are not internally deformed, they are included in the schist lithotype. Also within the mafic–ultramafic schist are good exposures of variably deformed pillowed metabasalt (*PAn*). This can be seen in areas 2 km south and 4 km southwest of Randell Bore, and 1 km north-northeast of Durack Well. In addition, pods and lenses of jasperoidal chert are, in places, associated with the volcanic rocks, and they may

represent, at least in some cases, hot spring chemical precipitates (*EAnc*).

The metabasaltic hyaloclastites (*EAnh*) are undeformed, dominantly of mafic composition, and have a spilitic character. Spilitic rocks are basaltic rocks that become altered through metasomatic exchange with seawater, thereby increasing their sodium content. The hyaloclastites on BRYAH have normative albite of up to 23 wt% and Na₂O content of up to 6 wt%.

Hynes and Gee (1986) reported on the petrochemistry and tectonic setting of the Narracoota metabasite rocks. They concluded that they have fairly uniform chemistry and are of mid-ocean-ridge basalt (MORB) affinity, although the original mafic volcanic rocks may have been emplaced through the rifting of continental crust. Hynes and Gee (1986) also noted the presence of ultramafic members (high-Mg basalts and komatiite). In the area 2 km northeast of Ravelstone, a texture described by Hynes and Gee (1986) as 'polygonal jointing' has been observed in the metabasalt, and appears to be a well-developed pencil cleavage.

#### **Actinolite schist and chlorite schist (*EAns*)**

Mafic-ultramafic schist (*EAns*) consisting of actinolite(–chlorite–clinozoisite) schist outcrops in the south-central part of BRYAH, forming an arcuate band (possibly an anticline structure; Gee, 1987) to the south of, and following the trends of, the Robinson Syncline and

the southern limbs of the Fraser Synclinorium. North of these structures, sparse outcrops of mafic schist lie just south and to the north of the Peak Hill Schist (Fig. 7). Within the schist are pods of less deformed or internally undeformed mafic volcanic rocks in which the previously mentioned pillow structures can be recognized (*EAn*). Overall, this large band forms a major anastomosing shear domain (Pirajno et al., 1995b). The dominant schistosity strikes approximately east or west-northwest, and dips steeply to the north and to the south. A number of quartz veins within this shear domain also strike east. Mafic-ultramafic schist was formed as a result of deformation and metasomatism of metabasite rocks along D₂ shear zones (see **Structure and metamorphism**). In most cases all original volcanic textures are obliterated, although in places, round or elongate chlorite aggregates are interpreted as original amygdaloids.

Mineral constituents of the mafic schist are actinolite, chlorite, and clinozoisite with minor amounts of calcite, pumpellyite, sericite, titanite, quartz, and relic albite. Ultramafic schist has a more simple and generally almost monomineralic mineralogy, consisting of actinolite–tremolite with retrogressed patches of pale-green chlorite. In zones of more intense deformation, chlorite- or epidote-dominated assemblages are present (chlorite schist and epidosite respectively). These minerals developed due to strong magnesium and calcium metasomatism, probably due to circulation of H₂O–CO₂ fluids (Pirajno et al., 1995b).



FMP 173

19.11.97

Figure 7. Typical outcrop of Narracoota Formation mafic schist. The scale bar has a 1 cm graduation

Fluid infiltration causes the breakdown of tremolite and clinozoisite to produce chlorite, calcite, and silica. The silica thus liberated is then channelled through shear zones, resulting in silicification and/or quartz veins (Pirajno et al., 1995b). An example of this situation can be seen in a breakaway 1.3 km east of the Wembley gold deposit (AMG 593480), where mafic schist and deformed pillow lavas display chlorite alteration and pervasive silicification near, and along, a west-northwesterly trending shear zone.

The mafic schist and pillow metabasalts are associated with metadolerite sills or dykes, autoclastic volcanic breccias, and vent breccia. A lenticular outcrop of metapyroxenite is present near Durack Well (AMG 690465). In places, mafic volcanoclastic rocks with well-preserved textures (Fig. 8) outcrop.

### **Metabasite (EAna)**

In the northern part of BRYAH, schistose metabasite (EAna) is present 5 to 8 km northeast of Peak Hill. It contains actinolite, arfvedsonite, calcite, diopside, epidote, and quartz. The alignment of actinolite and arfvedsonite defines the  $S_2$  schistosity, and therefore both these minerals were formed during pre- to syn- $D_2$ . Small crystals of diopside may be relics of the precursor lithology — possibly a gabbroic rock or a pyroxenite. The presence of arfvedsonite suggests either an original Na-rich rock or later sodic metasomatism during, or prior to,  $D_2$ .

### **Metadolerite dykes (EAnd)**

A metadolerite sheeted dyke complex (EAnd) lies north of the Robinson Syncline in the northeastern part of BRYAH. These rocks are associated with deformed pillow metabasalts. These units tend to be internally undeformed, but commonly form elongate bodies subparallel to the  $S_2$  foliation. They contain diopside, amphibole, clinozoisite, and minor amounts of olivine.

### **Metabasaltic hyaloclastite (EAnh)**

The metabasaltic hyaloclastites (EAnh) form a prominent outcrop area (partly covered by lateritic materials and colluvium) south of the Murchison River. These rocks probably represent a substantial thickness of mafic lava and hypabyssal material. A total thickness of 4 to 6 km is estimated by Hynes and Gee (1986) and Gee (1987). To the south, and outside BRYAH — on GLENGARRY (1:100 000) (Pirajno et al., 1997) — the metabasalts intercalate with sedimentary rocks of the Karalundi Formation. These metabasaltic rocks are interpreted as hyaloclastites: a term that denotes fragmentation, due to quenching, of lavas flowing in water or erupting under an ice sheet. This results in non-explosive fracturing and disintegration of the quenched lavas (McPhie et al., 1993; Fischer and Schmincke, 1984).

The metabasaltic hyaloclastites are albite normative (13 to 23 wt%), generally aphyric, and composed mainly of acicular crystals of actinolite (forming sheaves with



FMP 174

19.11.97

Figure 8. Photomicrograph showing pyroclastic texture (note relict shards in centre) in a mafic schist of the Narracoota Formation. GSWA 120367, plane-polarized light

plumose textures), epidote, minor amounts of carbonate, prehnite, quartz, titanite in a fine-grained groundmass of albite microlites, chlorite, and epidote. Overall, the preserved textures indicate quenched subaqueous basaltic lavas (Fig. 9). Coarse-grained equivalents (clinopyroxene and plagioclase laths) are present and they display ophitic to subophitic textures. North of the Mikhaburra (Holdens Find) gold deposit (AMG 568308) a small shaft has exposed a vesicular rock containing serpentinized olivine crystals set in a very fine altered matrix of actinolite — probably replacing pyroxene.

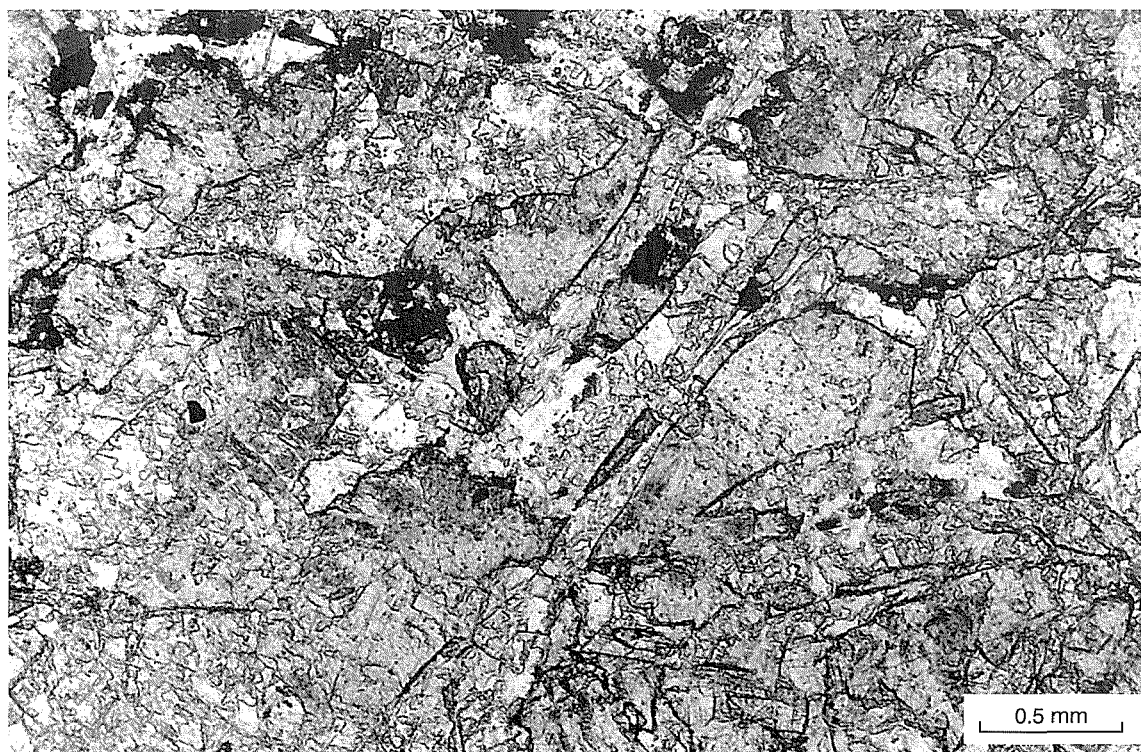
These metabasalts are generally unfoliated, massive, and with a characteristic brecciated or jigsaw-fit textured appearance outlined by epidote, carbonate, prehnite, and/or quartz along cooling joints. In places these cooling joints may form pseudo-pillow structures, and may be mistaken for pillow lavas (Hynes and Gee, 1986). Jigsaw-fit textures may also be seen at microscopic scale.

### ***Metabasaltic vent breccia (EAnx)***

In at least three localities volcanic breccia materials (EAnx) are present. The most important of these is 5 km north of Cashman (AMG 638317), in the southern part of BRYAH. The volcanic breccia is not exposed, but was intersected throughout 455 m of core from drillhole BD1, drilled by North Exploration in 1993 (McDonald, 1994). Outcrops of volcanic breccia are present at Cashman and 3 km west of the Peak Hill – Fortnum road junction. The nature of these angular, clast-supported, poorly sorted

blocks of basic volcanic material suggest that they are vent breccias. A good exposure can be seen at Cashman, along the track leading to the abandoned openpit (AMG 621270).

Drillhole BD1 (AMG 380380) was drilled to a depth of 520 m at an inclination of 70°S. It intersected clays and gravels to a depth of 65 m, followed by weathered mafic volcanic breccias to 96 m. Below this depth, to the end of the hole at 520 m, spectacular fresh near-vent facies material consisting of angular blocks and clasts of basaltic lava, tuff, and chert were intersected (Fig. 10). Crude bedding is present locally, as are thin layers of laminated or cross-laminated cherty material (possibly pyroclastic surge deposits). The hole bottomed in cross-laminated chert, which has been interpreted as pyroclastic surge and tuff deposits. The basaltic rocks include fine-grained, vesicular basalt, and feldspar-phyric and augite-phyric basalts. The phyric varieties are characterized by a feldspar-rich matrix, clinopyroxene granules, interstitial glass and chlorite, and opaque minerals (titanite or rutile). The feldspar phenocrysts are selectively altered to sericite, whereas the augite phenocrysts are fresh and exhibit distinct zoning. Vesicles are infilled (from rim to core) by albite, epidote, chlorite, and/or calcite. Minor sulfide specks (mainly chalcocopyrite) may be present in the vesicular basalt. Tuffs, characterized by fluidization (due to degassing) and/or eutaxitic textures, consist of glass shards and crystal and lithic fragments — all set in a devitrified and variably altered glassy matrix. Alteration phases are mainly chlorite,



FMP 175

19.11.97

**Figure 9. Photomicrograph of basaltic hyaloclastite showing cuneiform devitrified shards (now replaced by silica and sericite). GSWA 112643, plane-polarized light**





FMP 176

19.11.97

**Figure 10. Volcanic breccia intersected in diamond drillhole BD1. Clasts are predominantly of basaltic rocks, and the matrix exhibits albitic alteration**

calcite, quartz, and albite. Chalcopyrite blebs are present in places.

Hydraulic fracturing and veins of calcite, prehnite, quartz, and chlorite are abundant. One section between 200 and 360 m is characterized by albitic alteration (Na metasomatism), which imparts a reddish pink colouration to veinlets and patches where the albite is present.

As mentioned above, the fragmental mafic volcanic material in drillhole BD1 is interpreted as proximal-vent facies volcanic breccia. This vent facies material coincides with prominent magnetic and Bouguer gravity anomalies (Pirajno et al., 1995a). The magnetic anomaly, which is related to the presence of magnetite in pyroxene basalt, has a well-defined northeast-trending elliptical shape, and it could conceivably indicate the remnants of a major volcanic edifice. Magnetic modelling carried out by North Exploration suggests the presence of a body dipping 25 to 40° to the north (McDonald, 1994). The gravity anomaly is at the centre of a large regional gravity high, which underlies most of the area occupied by the Narracoota Formation. These anomalies are discussed further in **Aeromagnetic and gravity data**.

### **Jasperoidal chert (E_{Anc})**

Jasperoidal chert pods (E_{Anc}) are locally present within the Narracoota Formation. They are generally too small to be represented individually on geological maps. One pod is 1.5 km due south of Ruby Duffer Well in the southern part of BRYAH. These rocks consist of micro-crystalline quartz with hematite dustings. Windh (1992) investigated the chert pods in this region in some detail and geochemically differentiated them on the basis of their Ni/Cr ratios. She discriminated between jasperoidal syngenetic exhalative chert, silicified rocks, and silicified shear zone rocks. Several of these chert pods — like those in the Narracoota Formation, south of the

Peak Hill Schist in the northern part of BRYAH — are quartz mylonites (probably Windh's silicified shear zone rocks); others may be chemical precipitates deposited by hot springs.

### **Ravelstone Formation (E_{Ar})**

Outcrops of the Ravelstone Formation (E_{Ar}) are close to, and in contact with, mafic schist of the Narracoota Formation in the central part of BRYAH. The Ravelstone Formation, although metamorphosed, has no tectonite fabrics and consists of turbidite facies sedimentary rocks — mainly lithic and quartz wacke, and siltstone. The Ravelstone rocks were previously considered by McLeod (1970) and Gee (1979, 1987) to belong to the Thaduna Greywacke, for which the type area is some 100 km to the east-northeast on THADUNA (Pirajno and Adamides, 1997).

A good exposure, showing a disconformable contact between the base of the Ravelstone Formation and the top of the Narracoota Formation, is exposed in a river bed about 1 km due east of where the road to the Peak Hill mine meets the Ashburton Downs — Meekatharra road (AMG 647565). In this area the Ravelstone Formation has graded layers (immature subarkosic sandstone to siltstone) containing clear plagioclase, K-feldspar, sericitized lithic fragments, and angular quartz grains in a matrix of sericite and biotite. In addition, the siltstone contains euhedral crystals of tourmaline. Metamorphic brown-biotite and muscovite are abundant and replace feldspars, quartz, and lithic fragments. Samples collected in this area were used for U–Pb zircon dating (see **Geochronology**). Drillcore from the Harmony gold deposit shows that the contact between the base of the Ravelstone Formation and the top of the Narracoota Formation is interfingered, possibly due to shearing.

## Horseshoe Formation (PAh)

The Horseshoe Formation occupies a small area in the northwestern part of BRYAH, extending from the Ravelstone manganese deposit, north of the Peak Hill airstrip, to the northwestern boundary of the map sheet. This formation includes graded quartz wacke, manganeseiferous shale, garnetiferous biotite–chlorite schist, and garnetiferous iron-formation (PAh). The type area of the Horseshoe Formation is the Horseshoe Range, northwest of BRYAH, on PADBURY (Occhipinti et al., 1997a). A thickness of about 1000 m was estimated by Gee (1979). On BRYAH the Horseshoe Formation overlies the Narracoota Formation; however, the contact appears to be tectonic. Elsewhere, on JAMINDI (north of BRYAH), the Horseshoe Formation overlies the Ravelstone Formation, and the contact is gradational and conformable. The Horseshoe Formation underlies the Labouchere Formation of the Padbury Group. The nature of this upper contact appears conformable on BRYAH; however, Martin (1994) suggests that there is a regional unconformity between these units.

Structurally the Horseshoe Formation forms a broad syncline with its axis trending approximately east. The southern limb of this syncline is in sheared contact with rocks of the Narracoota Formation. In this area the Horseshoe Formation is complexly folded, with axes trending 070° — parallel to the shear zone.

The quartz wacke component of the Horseshoe Formation contains quartz, plagioclase, microcline, biotite, and muscovite — all as detrital minerals. The iron formation is made up of biotite, amphibole, chlorite, quartz, magnetite, and garnet.

About 1 km north of the Ravelstone manganese deposit, a reasonably good exposure of the Horseshoe Formation (AMG 700670) was examined in detail. A stratigraphic column for this locality is shown in Figure 11. This is a folded, upward-coarsening package about 350 m thick, which from base to top consists of quartz-lithic wacke with banded chert interbeds displaying a well-developed axial planar cleavage, quartz wacke with iron formation and shale interbeds, massive beds of coarse-grained quartz-lithic wacke intercalated with thin granular iron-formation, amphibole- and garnet-bearing granular iron-formation layers, and massive quartz-lithic wacke intercalated with thin iron-formation bands. The quartz-lithic wacke contains chert clasts, subangular quartz, fresh plagioclase crystals, biotite in a matrix of sericite, green chlorite, and iron-oxide grains. In places the cementing material is carbonate. Banded cherty material is composed of granular quartz aggregates, brown biotite, actinolite, and very fine carbonate-rich laminae (this rock is best classified as a quartz–biotite–actinolite schist). The granular iron-formation consists of granular aggregates of quartz and iron oxides with interstitial biotite and chlorite; syntectonic garnet porphyroblasts are present and are replaced in part by quartz and carbonate. Massive lithic wacke consists of a packed aggregate of angular quartz, feldspar, and chert grains; the matrix is volumetrically small and is made up of biotite, quartz, and sericite.

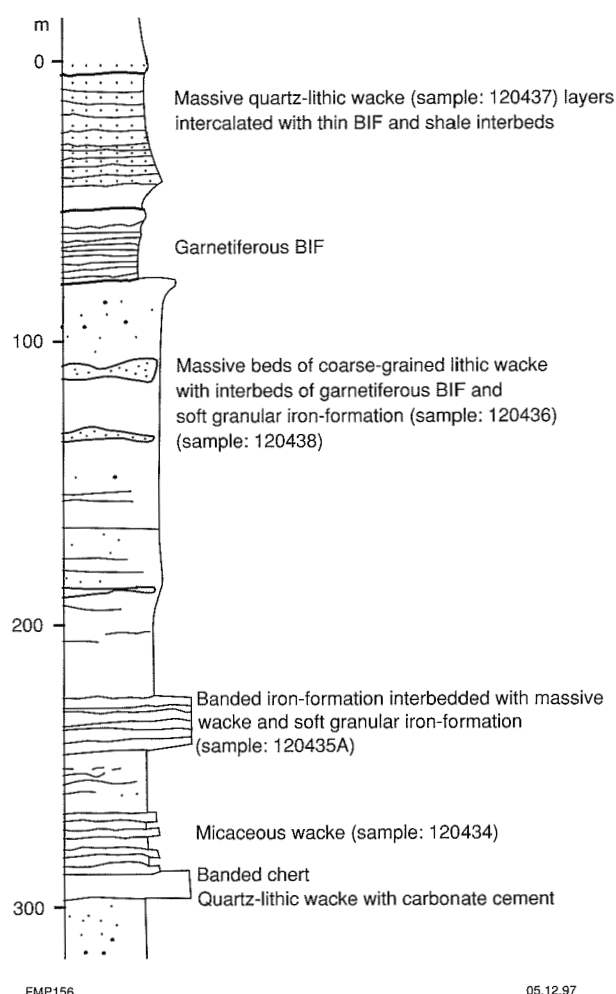


**Figure 11. Schematic stratigraphic column of the Horseshoe Formation, derived from an area of outcrops about 12 km west-northwest of the Peak Hill mine**

Garnetiferous iron-formation has dark laminae of quartz granules with interstitial actinolite–chlorite and iron oxides, and light-coloured microbands (1 cm) of quartz with actinolite–chlorite, iron oxides, and disseminated syn-late-tectonic garnet porphyroblasts. Garnet also forms porphyroblasts growing across microband boundaries.

## Padbury Group

On BRYAH the Padbury Group includes the Labouchere, Robinson Range, and Millidie Formations, and the Heines Member of the Wilthorpe Formation. The Padbury Group rocks are folded into tight synclines (Robinson Syncline and Fraser Synclinorium). The definition of the Padbury Group has been modified to include the Heines Member (Occhipinti et al., 1997a) — which incorporates part of the Wilthorpe Conglomerate of Gee (1979) — situated near the Heines Find gold prospect and Murphy Well areas. The Heines Member is a member of the Wilthorpe Formation, which includes the Wilthorpe Conglomerate of Gee (1979). On BRYAH the relationship between the Padbury and Bryah Groups is uncertain, owing to the

presence of extensive aprons of colluvial material. Gee (1979) and Martin (1994) have reported evidence of an unconformity between the Padbury and Bryah Groups. No unconformity was observed on BRYAH, and in the north the contact between the base of the Labouchere Formation and the top of the Horseshoe Formation appears to be conformable. It is possible that although this contact appears locally conformable, it may be regionally unconformable.

South of the Robinson Syncline the contact between the Heines Member and the underlying Narracoota Formation is faulted. This fault can be observed in the vicinity of Murphy Well (AMG 630506) and at the Heines Find gold prospect (AMG 829455). Elsewhere a thrust contact can be observed; for example, along the southern limb of the Fraser Synclinorium. Structural observations suggest that the Padbury group is older than the Earraheedy Group (which also directly overlies the Bryah Group).

The Padbury Group is characterized by BIF, granular iron-formation, ferruginous shale, and wacke.

### Labouchere Formation (*EPI*, *EPIi*, *EPIa*)

The Labouchere Formation (*EPI*) is present in the northwestern part of BRYAH and overlies the Horseshoe Formation. On BRYAH the Labouchere–Horseshoe contact is marked by a conglomeratic unit. The Labouchere Formation is estimated to be 5000 m thick (Gee, 1979), extending from Mount Labouchere (type area — MILGUN; Martin, 1994) to the Horseshoe Range — the southern continuation of which is in the northwestern part of BRYAH. Gee (1979) suggested that the Labouchere Formation conformably overlies the Horseshoe Formation (this is confirmed for BRYAH); although, Martin (1994), mapping in the type area, identified a regional unconformity at its base. It is considered possible that the Labouchere Formation is locally conformable and regionally unconformable over the Horseshoe Formation. Martin (1994) suggests that the top of the Labouchere Formation is marked by an unconformity, overlain by the Wilthorpe Formation, in the type area on ROBINSON RANGE.

On BRYAH the Labouchere Formation consists of a thick succession of upward-fining cycles up to 700 m thick. Each cycle consists of conglomerate or a coarse quartz–sericite–lithic wacke unit at the base, grading up through coarse- to fine-grained quartz–feldspar–lithic wacke, to sericitic siltstone, to iron-rich shale. These cycles, however, become increasingly coarser upward, so that there is regional upward-coarsening. The base of the top-most cycle begins with a quartz-pebble conglomerate. Minor and thin bands of iron formation (*EPIi*) are locally present as intercalations within the sedimentary units. A quartz arenite marker unit (*EPIa*), a few hundred metres thick, can be traced from MILGUN, through JAMINDI, and onto the northwestern part of BRYAH.

Sericite is abundant throughout most of the rocks of the Labouchere Formation. The quartz–sericite wacke is essentially a sedimentary breccia, and is composed of

subangular quartz grains embedded in a sericitized matrix with occasional large muscovite books and scattered small crystals of tourmaline and anatase. Quartz–feldspar–lithic wacke is made up of subangular quartz grains, polycrystalline quartz, K-feldspar, and plagioclase in a matrix of quartz, sericite, biotite, and minor detrital zircons.

## Wilthorpe Formation

### Heines Member (*EPwh*)

The Heines Member is considered part of the Wilthorpe Formation and includes those outcrops in areas south of the Robinson Syncline — at Heines Find (AMG 829455), Randell Bore, and 3.5 km northwest of Durack Well (AMG 630506) — previously mapped as Wilthorpe Conglomerate by Gee (1987).

The Heines Member (*EPwh*) consists of an upward fining sequence of sedimentary rocks with a polymictic conglomerate at its base, followed by clastic sedimentary units (sandstone to shale). The type area is near Durack Well. At this locality the Heines Member is folded into a syncline with its southern limb in faulted contact with the underlying Narracoota Formation. The northern contact here is obscured by the Cainozoic cover. The succession is about 600 m thick, although basal units may have been sheared off along the faulted contact. The basal polymictic conglomerate contains clasts of mafic lithic wacke, limestone, quartz arenite, and hematitic shale, all supported by a carbonate matrix. This is followed upward by a series of sandstone–shale units, with the shale component becoming volumetrically greater with stratigraphic height. The basal conglomerate of the Heines Formation contains no volcanic clasts of the underlying Narracoota Formation type, and this is taken as evidence that the contact with the latter formation is tectonic. The provenance of the various clasts in the basal conglomerate is not known. In the Heines Find area the Heines Member is overlain by the Robinson Range Formation.

### Robinson Range Formation (*EPr*, *EPrg*, *EPri*)

The Robinson Range Formation consists of a sequence of BIF (*EPri*) and ferruginous shale (*EPr*). In places the layers are contorted and/or brecciated. Granular iron-formation (*EPrg*) forms irregular lenses.

The mesostructure, microstructure, and petrology of the BIF are relatively simple (Fig. 12). In general, microbands (or laminae) ranging from less than 1 mm to 2–3 mm in thickness are made up of alternating assemblages of microcrystalline quartz(–iron oxides), greenish brown biotite – iron oxides, quartz grains – acicular crystals(–iron oxides), and quartz grains – iron oxides – biotite – acicular crystals. Commonly, the quartz grains – acicular crystals assemblage displays a polygonized texture suggestive of annealing due to metamorphism. The iron oxides can be hematite or magnetite. Incident light microscopy reveals that a primary titaniferous magnetite is replaced by hematite, which in turn, is replaced by goethite in the supergene

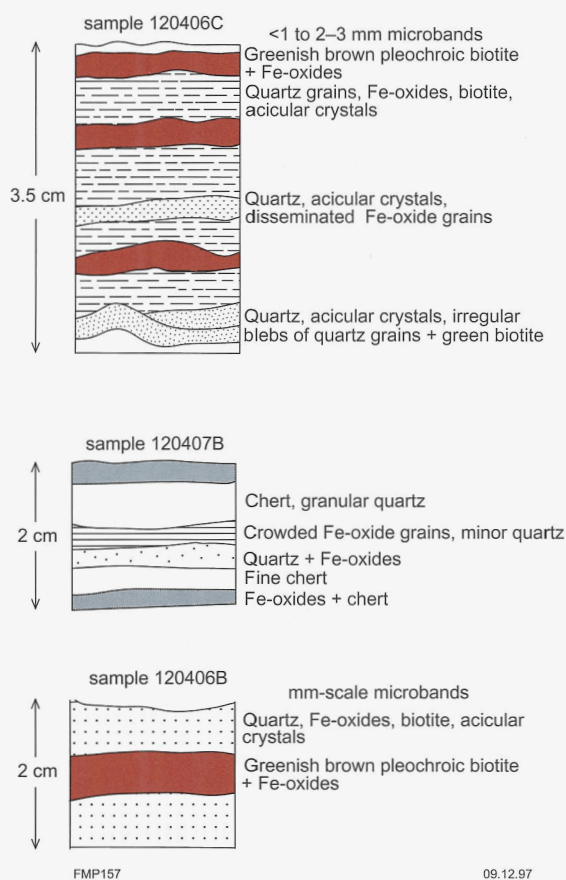


**Figure 12.** Examples of millimetre-scale microbands in the BIF of the Robinson Range Formation, as seen in thin section. GSWA 120406 and GSWA 120407

environment. The acicular crystals are weathered to iron oxides, but on the basis of their morphology they could be either stilpnomelane crystals or amphiboles. The biotite is porphyroblastic, with most crystallization occurring under conditions of peak metamorphism (see **Metamorphism**).

Granular iron-formation is characterized by a granular texture and the presence of elongate peloids 1–4 mm long. The peloids consist of microcrystalline chert, outlined by rims of iron oxides (hematite with inclusions of ilmenite). The chert peloids are enclosed in microcrystalline cherty or chalcedonic material. The peloids and chert make up bands about 1 to 1.5 cm thick, with a few laminae of a fine-grained chert – iron-oxides assemblage.

The ferruginous shale is composed of silt-sized quartz grains and iron oxides, with abundant interstitial biotite and minor amounts of disseminated euhedral tourmaline crystals. The latter were formed during either metamorphism or a hydrothermal event.

### Millidie Creek Formation (*EPm*)

On BRYAH the Millidie Creek Formation (*EPm*) is exposed in the northwest (at about AMG 506650) and consists of

ferruginous shales with a well-developed pencil cleavage, sandstone, and granular iron-formation.

## Earaheedy Group

The Earraheedy Group is represented on BRYAH by the Mount Leake Formation. This formation forms a series of elongate outliers, which unconformably overlie the Bryah and Yerrida Groups.

### Mount Leake Formation (*PEI*, *PEIc*)

Outliers of the Mount Leake Formation extend across the southern portion of BRYAH approximately parallel to, and south of, the Murchison River. The Mount Leake Formation generally trends easterly and dips shallowly to the north. One small outlier just north of the Murchison River is folded into an anticline.

The basal unit of the Mount Leake Formation is about 2 m thick, and consists of jasperoidal chert and green chert breccia (*PEIc*). This is followed upward by a ferruginous sandstone layer and layers of cross-bedded, locally glauconitic quartz arenite (*PEI*). The presence of glauconite is detectable by the pale-green colouration of the quartz arenite. The basal jasperoidal chert breccia may be representative of palaeoregolith material that developed on the unconformity surface above the Bryah Group prior to the deposition of the Mount Leake sedimentary rocks. Samples of the Mount Leake quartz arenite were used for U–Pb zircon dating (see **Geochronology**).

## Bangemall Group (*PM_y*, *PM_w*, *PM_b*, *PM_d*)

The Bangemall Group (Bangemall Basin; Muhling and Brakel, 1985) is present in the northeastern part of BRYAH. Most rocks of this group are very poorly exposed and are largely represented by shale and laminated chert of the Backdoor Formation (*PM_b*), which is unconformable on the Bryah Group. In the far northeastern corner of BRYAH, outcrops of the Calye Formation (quartz arenite — *PM_y*) and the Wonyugunna Sandstone (bedded arenite — *PM_w*) are present. An outcrop of undeformed basal conglomerate of the Bangemall Group that unconformably overlies shale of the Labouchere Formation has been assigned to the Wonyugunna Sandstone unit. This unit, which is a quartz-pebble conglomerate, was previously referred to as the Wilthorpe Conglomerate by Gee (1987). A small outcrop of a dolerite sill (*PM_d*) is also present on BRYAH.

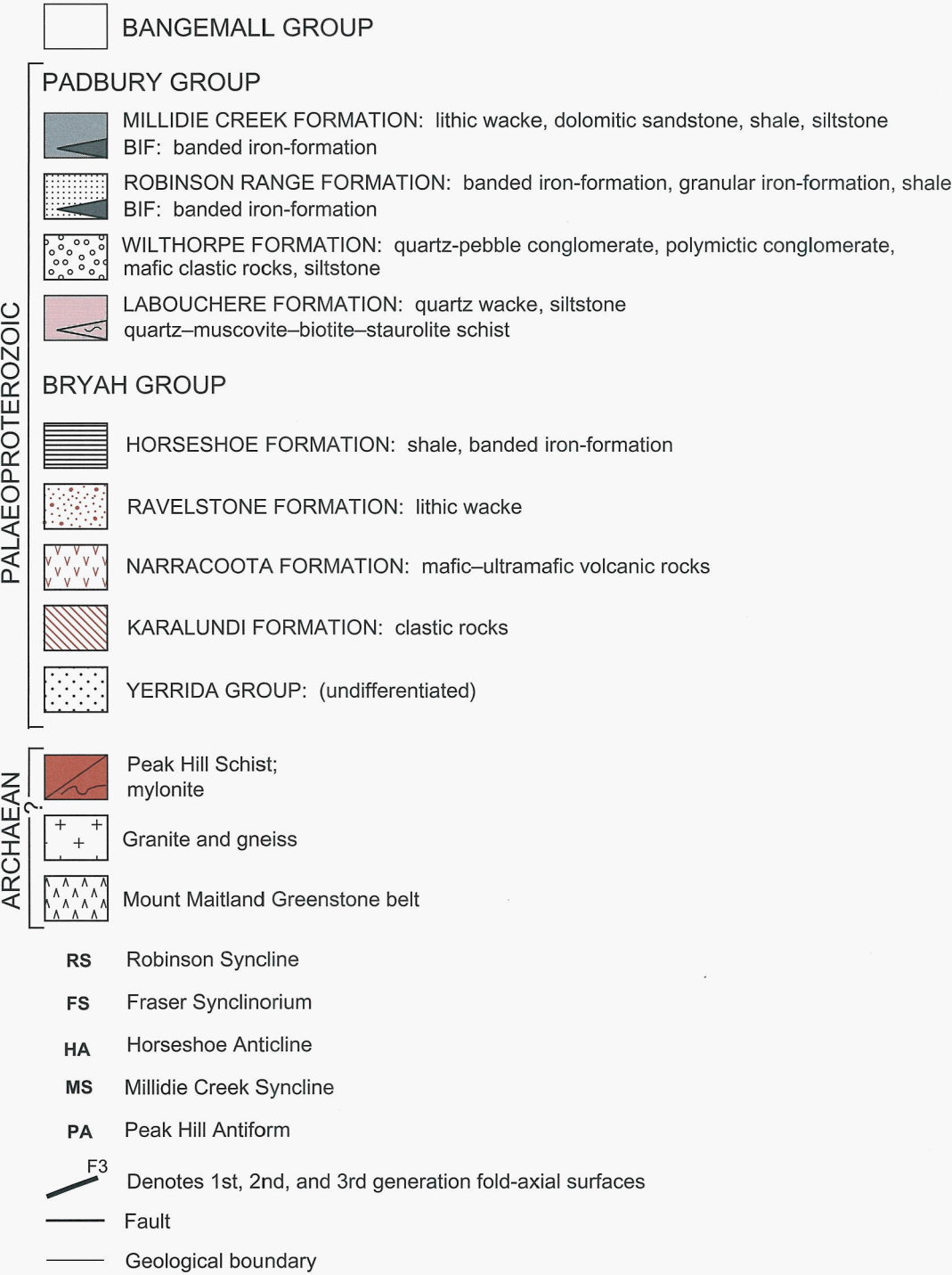
## Dolerite dyke (*Ed*)

A possible dolerite dyke (*Ed*) was detected by the aeromagnetic survey in the southeastern part of BRYAH. This dyke was probably emplaced along the Murchison Fault (see diagrammatic section on geological map).



Table 2. Relationship between diagnostic metamorphic minerals and deformation

Formation name	Rock type	Mineralogy	$pre-S_1$ $M_1$	$S_1$	$post-S_1$	$S_2-S_3$ $M_2$	$post-tectonic$
Peak Hill Schist	pelite	quartz	_____				
		biotite		_____			
		muscovite	_____				
		chlorite			_____		
		albite			_____		
		tourmaline			_____		
	chemical sediment	quartz	_____				
		spessartine	_____				
		magnetite	_____				
	calc-silicate	quartz	_____				
		epidote		_____			
		chlorite			_____		
		actinolite		_____			
		titanite		_____			
		magnetite					_____
Narracoota	psammite	quartz	_____				
		muscovite	_____				
		andesine		_____			
		opaques					_____
	metabasite	quartz					_____
		actinolite	_____				
		epidote	_____				
		chlorite			_____		
		sericite			_____		
		arfvedsonite			_____		
		titanite				_____	
		calcite					_____
	volcanic breccia	albite	_____				
		pumpellyite	_____				
Ravelstone	pelitic tourmalinite	quartz	_____				
		muscovite	_____				
		tourmaline			_____		
		garnet			_____		
		feldspar			_____		
	subarkosic wacke	quartz	_____				
		biotite					_____
		albite					_____
		sericite			_____		
		tourmaline					_____
Horseshoe	banded iron-formation	quartz	_____				
		biotite			_____		
		grunerite	_____				
		spessartine			_____		
		chlorite					_____
Robinson Range	banded iron-formation	quartz	_____				
		stilpnomelane			_____		
		biotite					_____



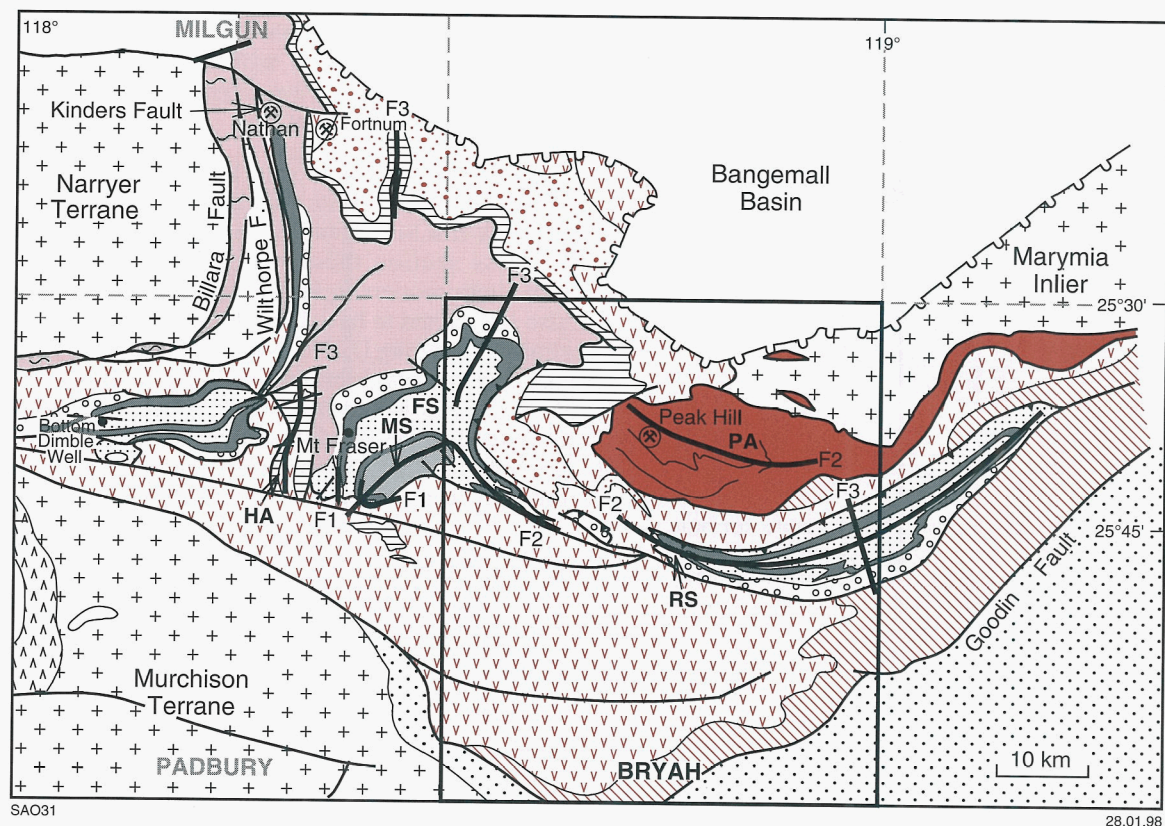


Figure 13. Simplified geology of the Padbury and Bryah Basins showing major fold and fault structures (legend is on opposite page). Modified from Occhipinti et al. (1996)

## Structure and metamorphism

Ocean-floor metamorphism affected the mafic volcanic rocks of the Narracoota Formation following their emplacement in an oceanic rift setting. Subsequently, deformation and regional prograde and retrograde greenschist facies metamorphic episodes occurred, probably as a result of the collision between the converging Yilgarn and Pilbara Cratons (Capricorn Orogeny; 2.0–1.8 Ga). This affected the Bryah and Padbury Groups, the Peak Hill Schist, the Marymia Inlier, and the Narryer Gneiss Complex. On BRYAH, three deformation events ( $D_1$ ,  $D_2$ , and  $D_3$ ) together with two metamorphic episodes ( $M_1$  and  $M_2$ ) are recognized. To the east, the volcano-sedimentary sequence of the Yerrida Group is much less deformed, and shows little or no evidence of metamorphism.

## Structure

Major fold structures on BRYAH are the Robinson Syncline, the Fraser Synclinorium, and the Peak Hill Antiform (Fig. 13). The Robinson Syncline and Peak Hill Antiform are interpreted as  $F_2$  folds that have been refolded during a later deformation event ( $D_3$ ) so that they became doubly plunging structures. In addition to this, an earlier deformation event ( $D_1$ ) caused folding, shearing, and faulting. These early folds can be observed in both the Peak Hill Antiform and Robinson Syncline, and  $D_2$

shear zones can also be observed in the Peak Hill Antiform. The unusual shape of the Fraser Synclinorium probably reflects a complex fold interference pattern, which formed due to overprinting of the three folding events in the area.

North of the Murchison River, rocks of the Mount Leake Formation are folded into an open anticline with its axis trending east. A major northeast-trending fault (Goodin Fault; Fig. 1) separates the Bryah and Yerrida Groups. On BRYAH, the Goodin Fault in the southeast is interpreted as a northwesterly dipping thrust that developed as a result of the collision between the Bryah and Yerrida Basins, possibly during  $D_2$ .

### $D_1$ structures

The first deformation ( $D_1$ ) involved folding, the formation of a schistosity, mylonitization, and faulting. However, because  $D_1$  structures were pervasively overprinted by  $D_2$  structures,  $F_1$  folds are rarely observed. The second deformation resulted in the reorientation of  $D_1$  structures and the development of folds, faults, and major shear zones.

The first deformation event produced layer-parallel folds,  $S_1$  schistosity, faults, and mylonites. The  $F_1$  folds are locally observed in the  $F_2$  fold-hinge zones of the quartz blastomylonites of the Peak Hill Schist, in the vicinity of the Peak Hill mine. Here the folds are small



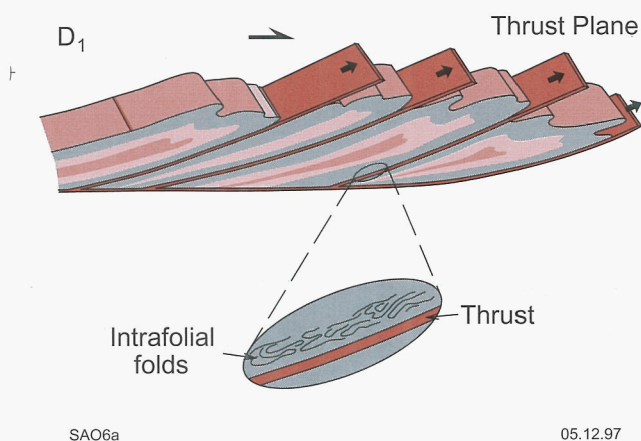


**Figure 14.** Sketch illustrating the possible formation of  $D_1$  structures, including subhorizontal to recumbent  $F_1$  folds and faults, via a fold-thrust belt; inset shows intrafolial folds in quartz blastomylonite from the Peak Hill Schist

scale, rootless, and isoclinal, and plunge shallowly towards the east. In addition, metre-scale  $F_1$  folds are observed in the hinge zone of the Robinson Syncline, north of Tank Well and northeast of Randell Bore. These folds are tight to isoclinal, and have shallow plunges to the east or west. It is possible that the Peak Hill Schist was previously deformed, but subsequently overprinted during  $D_1$  and  $D_2$ . The  $F_1$  folds are interpreted as originally being subhorizontal (Fig. 14).

On BRYAH, no evidence of  $D_1$  was observed in the mafic schist south of the Robinson Syncline, or in the metabasaltic hyaloclastites and rift-fill sedimentary rocks south of the Murchison River.

Quartz blastomylonites and the Crispin mylonite form folded continuous units within the Peak Hill Schist. The proximity, uniformity, and internal structure of these units suggest that they may be  $D_1$  shear zones that were refolded during the later deformation events. The original nature and orientation of these shear zones is not known (see discussion below).

The Crispin mylonite consists of quartzite pebble- and boulder-sized clasts in a sericite-quartz-rich matrix, and has the appearance of a conglomerate. For that reason it was mapped by Gee (1987) as the Crispin conglomerate. However, mesoscopic and microscopic structures indicate that it is a mylonite. Both the quartzite clasts and the matrix contain a mylonitic fabric. The Crispin mylonite is interpreted as a 'pseudo-conglomerate' (Raymond, 1984a,b) formed by shearing, probably along, or close to, a fault plane that separated an arkosic unit from a quartz arenite. If this is correct, then, with progressive shearing and metamorphism, the more competent quartz arenite may have undergone brittle deformation, whilst the less competent arkosic unit may have deformed in a ductile manner. The competency contrast between the two units would lead to the fragmentation and formation of boudins of quartz arenite within the ductile deforming arkose.

With continued shearing, the mylonitic quartz sandstone blocks became isolated within mylonitized arkosic sediments — representing a type of tectonic melange zone (Raymond, 1984a,b).

Like the Crispin mylonite, the quartz blastomylonites form arcuate lenses within the quartz-muscovite schist of the Peak Hill Schist, and are refolded by  $F_2$  and  $F_3$  folds. In cross section these rocks contain isoclinal and sometimes rootless  $F_1$  folds (Fig. 14). The mylonites are also interpreted to have been deformed in a ductile high-strain zone during  $D_1$ . No indicators were observed during mapping to allow determination of the sense of movement during  $D_1$ . However, the Peak Hill Schist is assumed to be older than the Bryah Group rocks in the area and it is possible that they were thrust onto the Bryah Group, probably in a compressional regime.

## $D_2$ structures

The second deformation ( $D_2$ ) produced upright large-scale  $F_2$  folds. The  $F_2$  folds display a variety of orientations. The Robinson Syncline, in the central part of BRYAH, is a steeply inclined, easterly trending, tight isoclinal fold. North of Tank Well the fold plunges shallowly to the east. Northwest of Randell Bore it shallowly plunges both to the east and west, forming a basin structure, as a result of refolding during  $D_3$ .

In the northern part of the Bryah Basin, on BRYAH, small-scale  $F_2$  folds have steeper plunges (up to  $60^\circ$ ) and trend approximately east. Locally,  $L_2$  extension lineations, defined by the alignment of muscovite, developed during  $D_2$ . These are subparallel to the  $F_2$  fold axes that plunge to the east and the west (due to refolding) indicating that east-west extension, coupled with north-south compression, took place during  $D_2$ .

The  $D_2$  structures include folds, faults, and shear zones. The  $D_1$  structures were refolded and, locally,  $S_2$  schistosity developed; for instance, in the  $D_2$  shear zone south of the Robinson Syncline. The  $D_2$  faults and shears have been observed in the Doolgunna Formation at Goodins Find; in the Padbury Group north of Trudgeon Well; at the boundary between the Padbury Group and the Narracoota Formation in the Randell Bore area; and north of the Jubilee area at the boundaries between the Peak Hill Schist, the Narracoota Formation, and the Horseshoe Formation. The relative age of other faults recognized in the area — for example, the faults interpreted between the Robinson Range and Narracoota Formations, and the faults around the Robinson Syncline and Fraser Synclinorium — is uncertain. These faults may be  $D_1$  structures that have been refolded during  $D_2$ . It is also possible that some of these are  $D_1$  faults that were reactivated during  $D_2$ .

Metasomatizing fluids were channelled along the  $D_2$  shear zones. On BRYAH, one such zone lies to the south of the Robinson Syncline and the Fraser Synclinorium. Here a regional anastomosing shear zone formed in the basaltic rocks of the Narracoota Formation (Pirajno et al., 1995b). This shear zone cuts the interpreted  $D_1$  fault that separates the Padbury Group and Narracoota Formation near the hinge zone of the Robinson Syncline. A fault



along the southern limb of the Fraser Synclinorium extends into the  $D_2$  shear zone mentioned above. It is likely, in this case, that this fault is a folded  $D_1$  thrust that may have been reactivated, and extended across the fold during  $D_2$ . Another shear zone cuts the southern limb of the Heines Syncline, which lies between the Robinson Syncline and Fraser Synclinorium. These shear zones are steeply dipping and the sense of shear could not be determined.

During  $D_2$  the sedimentary rocks and metabasaltic hyaloclastites south of the Murchison River reacted in a brittle manner. This may be due to these rock units being more competent than those north of the Murchison River and/or being at a higher structural level during the second deformation event. The  $D_2$  fabrics in this area include a crude fracture cleavage and the local development of a slaty cleavage.

### **$D_3$ structures**

The third deformation ( $D_3$ ) was a regional faulting and folding event that took place during or after the deposition of the Mount Leake Formation. Small-scale open  $F_3$  folds have steeply plunging fold axes with northerly trending fold-axial surfaces. No pervasive  $S_3$  cleavage is evident. Large-scale  $D_3$  folds refolded the  $D_2$  structures, resulting in the development of doubly plunging  $F_2$  folds in the Robinson Syncline and in the antiformal structure in the Peak Hill area.

It is possible that the intensity of  $D_3$  increased towards the western margin of the Bryah Basin to form tighter  $F_3$  folds and contributed to the development of the complex fold interference pattern observed in the Fraser Synclinorium.

### **Discussion and interpretation**

Martin (1994) proposed that the Padbury Group was deposited in a foreland basin on the Glengarry Basin, as defined by Gee and Grey (1993). This area corresponds with what is now called the Bryah Basin (Pirajno et al., 1995a; Pirajno and Occhipinti, 1995; Pirajno, 1996; Occhipinti et al., 1996). He suggested that through time, continued convergence of the fold-thrust belt and the foreland led to the formation of isoclinal folds in the region. These are the  $F_2$  folds with steeply dipping axial surfaces recognized on BRYAH. The upright nature of these folds indicates they did not form during thrust propagation, because such folds would have shallower dipping fold-axial surfaces (less than  $45^\circ$ ). However, it is probable that the  $F_1$  folds, faults, and shear zones in the region, that are interpreted to have originally been shallow dipping structures, may have developed in this environment. Thornett (1995) observed probable duplex structures below the Peak Hill mylonite in the Fiveways Pit at the Peak Hill mine. This supports the assumption that  $D_1$  was a compressional event that involved thrusting.

The main structural fabric within the Peak Hill Schist is the  $S_1$  schistosity. This appears to be a layer parallel schistosity that is subparallel to the  $F_1$  (isoclinal to

rootless) folds in the area. This  $S_1$  fabric is also observed in thin section in the BIF of the Horseshoe Formation, where it is subparallel to bedding. This schistosity is defined by the alignment of biotite and muscovite, and is the peak metamorphic fabric in the area. This peak metamorphic fabric is assigned to the first metamorphic episode ( $M_1$ ).

Granitoid rocks of the Marymia Inlier, on BRYAH, contain a foliation subparallel to that in the adjacent Peak Hill Schist. This suggests either a reoriented earlier Archaean fabric or a Proterozoic fabric. It is likely, however, this fabric developed during the Proterozoic and the  $D_1$  deformation event.

## **Metamorphism**

### ***Ocean-floor metamorphism of metabasaltic hyaloclastite rocks***

Hydration of mafic igneous rocks is commonly the result of interaction with water (usually seawater) soon after, or during, deposition. Although the primary igneous textures are normally preserved, a number of mineralogical and chemical changes take place. The mafic rocks metamorphosed in this way are also known as spilites (Hughes, 1982 and references therein). Spilitic rocks therefore are characterized by varying amounts of albite, actinolite-tremolite, chlorite, and epidote depending on the range of temperatures and pressures. In ocean-floor metamorphism, seawater penetrates through the mafic rocks, is heated, and becomes a hydrothermal solution. This causes mass transfer of Mg,  $SO_4^{2-}$ , Na, and Cl from seawater to the mafic rocks, while leaching and mass transfer of K, Rb, Ca, Ba, Cu, Fe, Mn, Zn, and Si take place from the mafic rocks to the solution.

On BRYAH, lithologies of the Narracoota Formation that best show the effects of ocean-floor metamorphism are the metabasaltic hyaloclastites, which lie south of the Murchison River. The metamorphic mineral phases of these rocks include actinolite-tremolite, chlorite, epidote, albite, pumpellyite, titanite, prehnite, calcite, and zeolite. These mineral phases are characteristic of greenschist to zeolite-pumpellyite facies. No attempt was made to discriminate between specific mineral assemblages in order to identify greenschist facies zones from zeolite-pumpellyite facies zones. The primary mineralogy is rarely preserved, but where it is present the chief mineral components are clinopyroxene and plagioclase.

Retrograde metamorphism, represented mainly by chlorite overprinting, occurred along discrete shear zones (e.g. Cashman area), which are also associated with gold and copper-gold mineralization.

North of the Murchison River the Narracoota Formation contains mafic and ultramafic schists. These are derived from the deformation and metamorphism of pillow lavas and associated dykes. They are essentially metamorphosed under conditions of regional greenschist facies metamorphism and metasomatism, which overprints the ocean-floor metamorphism.

**Table 3. Prograde metamorphic assemblages of the Bryah Group and possible precursor rocks**

<i>Rock types</i>	<i>Prograde assemblages</i>	<i>Accessory minerals</i>
Pelitic rocks	chlorite–biotite–muscovite–quartz chlorite–garnet–biotite–quartz carbonate–biotite–muscovite–K-feldspar–plagioclase–quartz	ilmenite graphite
Psammitic rocks	zoisite–biotite–plagioclase–quartz zoisite–chlorite–biotite–quartz green amphibole–epidote–biotite–plagioclase muscovite–quartz	magnetite–titanite
Carbonate rocks	calcite–dolomite–chlorite–muscovite–biotite–quartz	rutile
Mafic rocks	colourless amphibole–chlorite–biotite–quartz green amphibole–epidote–chlorite–quartz–carbonate green amphibole–epidote–chlorite–albite–quartz–carbonate	magnetite–titanite titanite graphite
Ultramafic rocks	colourless amphibole–chlorite–talc	spinel

Modified from Thornett (1995)

### **Regional prograde and retrograde metamorphism**

The relationships between metamorphic mineral growth and deformation on BRYAH are summarized in Table 2. The first metamorphic episodes accompanied  $D_1$ . This was a prograde regional metamorphic event that produced greenschist facies assemblages; although, locally, amphibolite facies assemblages have also been recognized. The second metamorphic episode ( $M_2$ ) was retrogressive, and associated with metasomatism in high-strain zones during  $D_2$ .

Relationships between metamorphic minerals and the  $S_1$  and  $S_2$  fabrics allow metamorphic assemblages within metabasite rocks (Narracoota Formation), calc-silicate and pelitic rocks (Peak Hill Schist), turbidites (Ravelstone Formation), and BIFs (Robinson Range and Horseshoe Formations) to be ascribed either to  $M_1$  or  $M_2$  (Table 2).

Greenschist facies mineral assemblages are distributed in the northeastern part of BRYAH, with the metamorphic facies changing to the south — across the Murchison River — where the metabasite rocks preserve the imprint of ocean-floor metamorphism (see previous section). The BIF of the Robinson Range Formation shows a marked increase in metamorphic grade, from DOOLGUNNA in the east, westward to BRYAH, with the biotite-in isograd lying along the Robinson Syncline, about 5 km east of the eastern edge of BRYAH. The presence of biotite and muscovite in the Ravelstone Formation subarkosic wacke suggests that biotite–muscovite formed at the expense of K-feldspar and chlorite within the mid-greenschist facies (350–400°C; Butcher and Frey, 1994, p. 203).

Thornett (1995) suggests that amphibolite facies grade was reached during  $D_1$  in the Peak Hill Schist. Results of Thornett's studies on geothermometry and geobarometry revealed temperatures of between 500 and 620°C for a peak prograde metamorphism, and 6.5 to 7 kbar for the minimum pressure of the prograde assemblages. These prograde assemblages are

summarized in Table 3. The results indicate that these rocks reached amphibolite facies during prograde metamorphism; however, these are based on a few drillcore samples from the Peak Hill mine area. The amphibolite facies assemblages (Table 3) reported by Thornett (1995) are not typical for the Peak Hill Schist.

The second metamorphic episode ( $M_2$ ) involved the retrogression and metasomatism of metamorphic mineral assemblages developed during  $M_1$ . During  $M_2$ , hydrothermal alteration also took place (discussed later in **Mineralization**). On BRYAH, mineral assemblages formed during  $M_2$  are only observed in high-strain zones, where the  $S_2$  schistosity is well developed. These include a domain of well-developed  $D_2$  shear zones south of the Robinson Range Formation synclines, where pervasive retrogression of metabasalt to actinolite–chlorite schist is recorded (Pirajno et al., 1995b). In the Mount Pleasant openpit the growth of albite porphyroblasts and the development of chlorite (at the expense of biotite and epidote) also took place during  $M_2$ .

The metamorphic assemblages of the Peak Hill Schist are given in Table 4. Chlorite commonly replaces biotite and epidote. Sericite–muscovite also overprints prograde biotite. Other minerals that crystallized during

**Table 4. Metamorphic assemblages of the Peak Hill Schist and possible precursor rocks**

<i>Precursor rock type</i>	<i>Metamorphic assemblage</i>
Pelite	quartz–muscovite–sericite–biotite(–tourmaline–magnetite)
Calc-silicate	epidote–chlorite–biotite–muscovite(–albite–calcite–quartz)
Psammitic	quartz–muscovite–feldspar
Chert	quartz–muscovite–garnet–magnetite–grunerite

M₂ include epidote, arfvedsonite, biotite, albite, carbonate, tourmaline, apatite, and titanite. As mentioned above, albite porphyroblasts are abundant in the Mount Pleasant pit (see Fig. 26, page 32). The concentration of albite poikiloblasts in this area is confined to high-strain zones and they commonly overprint the S₂ schistosity, indicating they crystallized late in M₂. The presence of albite may be due either to an influx of sodium-rich fluids, or to sodium contained in the protolith (Watkins, 1983; also see discussion in **Mineralization**).

In the mineralized zones (see **Mineralization**), chlorite, biotite, tourmaline, apatite, titanite, and carbonate are commonly present in and around veins and fractures, and between grain boundaries of the dominant rock-forming minerals of a particular unit. Green (hydrothermal) biotite crystallized as randomly oriented porphyroblasts within a pelite of the Peak Hill Schist (Fig. 27, page 33). In addition, some biotite has broken down to form chlorite. Tourmaline commonly overprints the dominant schistosity in the pelites of the Peak Hill Schist.

Microprobe analyses indicate that the tourmaline is elbaite. This suggests that boron may have been derived from the sediments, and transported and concentrated in high-strain zones during M₂.

## Volcanic geochemistry

Averages of major, trace, and rare-earth elements from whole-rock analyses of metabasite rock samples collected during the present work are given in Tables 5 and 6. The original data were used to characterize the geochemistry of the volcanic rocks of the Narracoota Formation in an attempt to better define the rock types, as well as to gain an insight into the nature of the parent magma(s) and the tectonic setting.

## Major and trace elements

All metabasites of the Narracoota Formation (ultramafic and mafic schist, and metabasaltic hyaloclastite) are of subalkaline tholeiitic affinity (Fig. 15). They have restricted silica contents ranging from 46 to 54 wt% (Fig. 16). The ultramafic schist is hypersthene and olivine normative, with Mg contents ranging from 15.3 to 22.7 wt% and magnesium number (Mg#, defined as MgO/(MgO + FeO²⁺)) ranging from 80.97 to 82.83. The mafic schist is hypersthene normative, with lower Mg contents (<15 wt%) and Mg# ranging from 49.8 to 70.81. The basaltic hyaloclastite is albite and clinopyroxene normative, and has Mg contents of less than 10 wt% and Mg# of between 48.22 and 61.07. Ultramafic schist, mafic schist, and metabasaltic hyaloclastite can also be differentiated in terms of their Cr, Ni, and Cu abundances. Figure 17 highlights the differences between the metabasites in terms of their Ni/Cu ratios and Cr abundances.

The Jensen (1976) cationic plot (Fig. 18) is particularly suitable for subalkaline and metamorphosed volcanic rocks. From this figure it can be seen that the metabasites

**Table 5. Averages of major- and trace-element analyses of the Narracoota Formation**

Major and trace elements	Hyaloclastite (9) ^(a)	Mafic schist (13)	Ultramafic schist (5)
Weight percentage			
SiO ₂	50.07	50.40	48.54
TiO ₂	0.80	0.48	0.17
Al ₂ O ₃	14.07	14.32	7.74
Fe ₂ O ₃	3.19	3.43	2.35
FeO	7.68	5.56	5.82
MnO	0.18	0.15	0.14
MgO	7.49	7.42	20.44
CaO	10.88	12.57	7.78
Na ₂ O	2.10	1.91	0.93
K ₂ O	0.33	0.05	0.03
P ₂ O ₅	0.08	0.04	0.01
LOI	3.49	3.18	5.92
<b>Total</b>	<b>100.36</b>	<b>99.51</b>	<b>99.87</b>
Parts per million			
Ag	0.34	0.81	0.84
As	0.05	1.23	1.80
Au (ppb)	2.44	2.30	1.60
Ba	119	78	32
Bi	0.06	1.15	1.40
Cd	0.01	1.20	1.04
Ce	1.71	2.83	1.76
Cr	140	490	2 309
Co	37	36	82
Cu	114	79	30
Ga	12.8	9.1	4.86
La	0.12	2.88	3.62
Mo	0.03	15.2	0.58
Nb	0.37	3.03	2.04
Ni	110	207	1 054
Pb	0.61	1.65	1.44
Pd (ppb)	2.0	7.9	6.66
Pt (ppb)	2.0	9.0	7.66
Rb	5.39	0.98	1.12
Sb	0.02	1.46	1.22
Sc	24	31	24.5
Sn	0.06	1.15	1.0
Sr	165	105	19.1
Th	0.50	0.92	0.60
U	0.01	0.52	0.44
V	264	234	131
Y	18.3	16.8	10.6
W	0.50	2.08	2.93
Zn	86	67	62
Zr	60	36	12.2
<b>Mg#</b>	<b>55.71</b>	<b>59.25</b>	<b>82.1</b>

Trace elements in ppm except where stated otherwise

Analyses were performed at the Chemistry Centre of the Department of Minerals and Energy Co., Cr, Cu, Ni, V, Zn were determined by ICP-AES following a mixed acid solution

Major elements were determined by XRF after samples were incorporated into a borate glass disk or a pressed powder

(a) Numbers in parentheses denote number of samples

LOI loss on ignition

Mg# Mg number (MgO/(MgO + FeO²⁺))

of the Narracoota Formation fall within the high-magnesium tholeiite (HMT), basaltic komatiite (BK), and peridotitic komatiite (PK) fields. A compositional gap is apparent between the HMT-BK and the PK. This feature is also shown in the total-alkali versus silica (TAS)



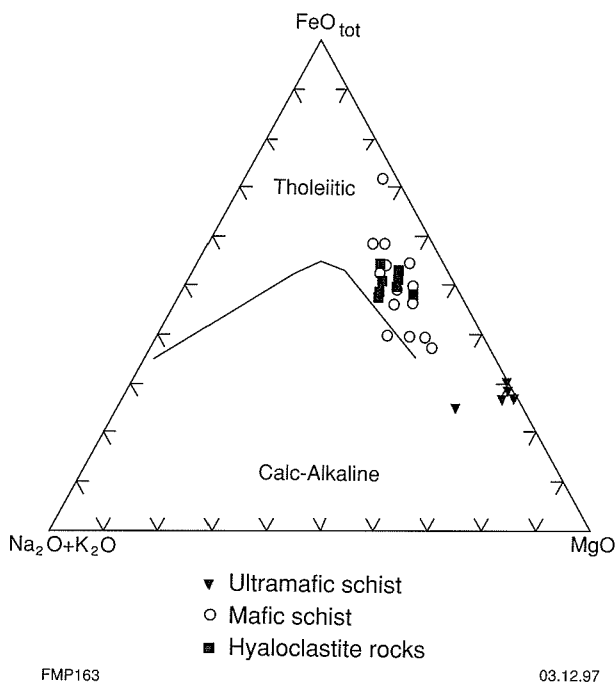


Figure 15. Triangular plot of  $(\text{Na}_2\text{O} + \text{K}_2\text{O}) - \text{FeO}_{\text{tot}} - \text{MgO}$ , after Irvine and Baragar (1971), illustrating the tholeiitic composition of the Narracoota Formation volcanic rocks

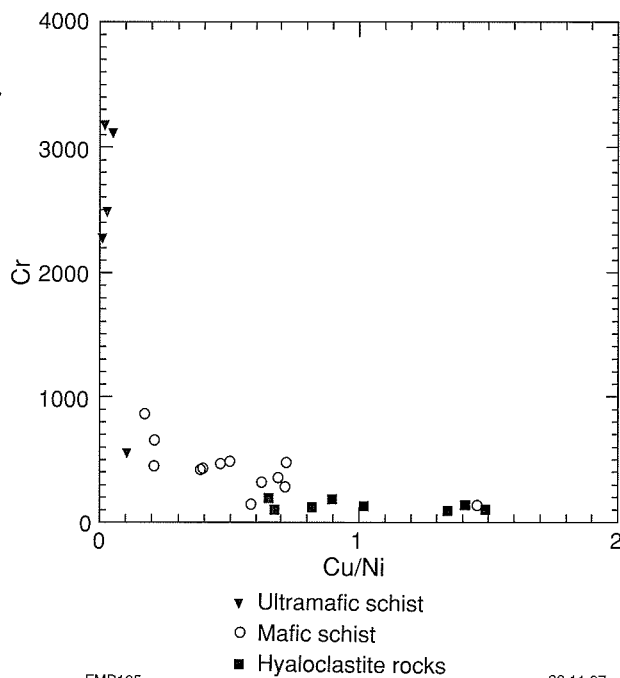


Figure 17. Cr versus Cu/Ni diagram illustrating the compositional differences between metabasites of the Narracoota Formation

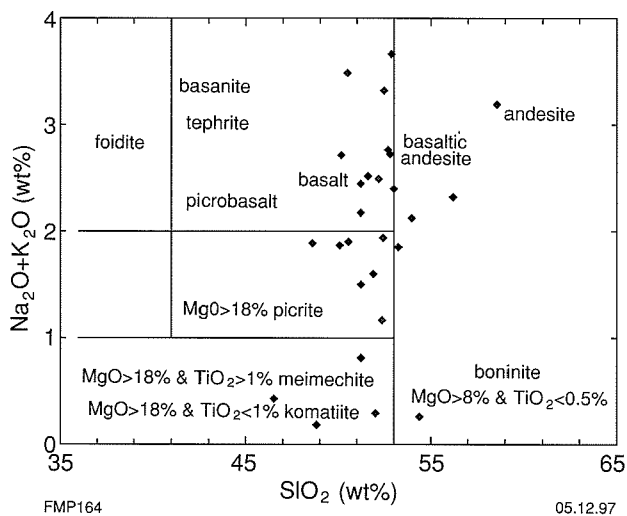


Figure 16. Position of the Narracoota Formation volcanic rocks on the total-alkali versus silica (TAS) diagram of Le Maitre (1989)

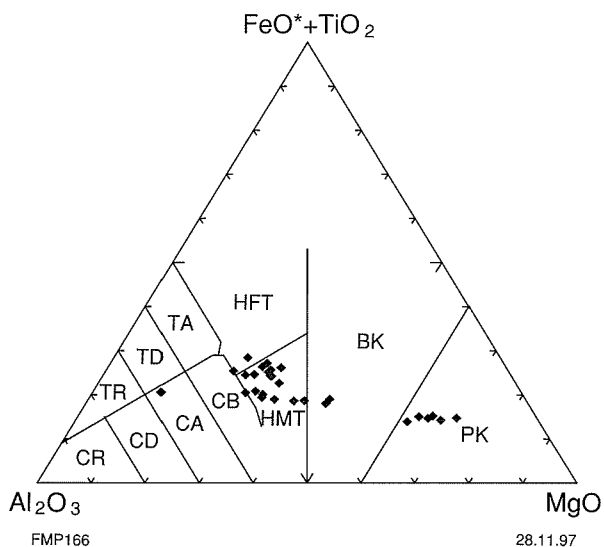


Figure 18. Jensen (1976) cationic plot of Narracoota Formation rocks showing the range of composition from mafic to ultramafic. PK: peridotitic komatiite, BK: basaltic komatiite, HMT: high-magnesium tholeiite, HFT: high-iron tholeiite, CB: calc-alkaline basalt, CA: calc-alkaline andesite, CR: calc-alkaline rhyolite, TA: tholeiitic andesite, TD: tholeiitic dacite, TR: tholeiitic rhyolite

Table 6. Rare-earth element representative analyses of the Narracoota Formation

Sample number	104256h	112643h	116485h	116487h	116493h	116501h	104393s	112601s	116477s	120369s	120373um	120432um
	Parts per million											
La	3.5	3.6	3.5	4.8	3.4	1	1.1	1.4	10.8	12.53	1.47	1.34
Ce	8.3	9	8.3	12.2	8.5	2.3	2.3	3.1	23.4	33.41	3.08	1.89
Pr	1.3	1.2	1.1	1.7	1.2	0.4	0.4	0.5	3.2	4.73	0.19	0.11
Nd	5.7	5.7	5.1	7.5	5.4	1.9	2.3	2.4	13.8	18.87	1.21	1.15
Sm	1.5	1.5	1.4	2.1	1.6	0.7	0.8	0.9	3.9	4.98	0.42	0.77
Eu	0.8	0.9	0.7	0.9	0.8	0.4	0.6	0.3	1.4	1.32	0.05	0.12
Gd	2	2.3	1.7	2.4	1.8	1.2	1.6	1.6	3.8	5.63	0.62	0.85
Tb	0.4	0.4	0.4	0.5	0.4	0.3	0.3	0.3	0.9	0.96	0.13	0.18
Dy	2.4	2.7	2.4	3.4	2.6	2.1	2.4	2.5	5.3	4.89	0.99	1.27
Ho	0.5	0.5	0.5	0.7	0.5	0.5	0.5	0.6	1.1	1.06	0.23	0.32
Er	1.6	1.8	1.5	2.1	1.6	1.8	1.8	2	3.2	2.97	0.73	0.9
Tm	0.2	0.2	0.2	0.3	0.2	0.3	0.3	0.3	0.4	0.45	0.05	0.05
Yb	1.5	1.5	1.4	1.8	1.4	1.7	1.7	1.9	2.9	2.47	1.09	1.2
Lu	0.2	0.2	0.2	0.3	0.2	0.3	1.3	0.3	0.4	0.48	0.13	0.15
La/Yb _{CN}	1.56	1.605	1.672	1.783	1.624	0.393	0.433	0.493	2.49	3.392	0.902	0.747
Eu/Eu*	1.385	1.669	1.3	1.17	1.3	1.48	1.73	0.735	0.956	0.685	0.31	0.43

Analyte concentrations were quantified using ICP-MS after a mixed acid solution  
Analyses were performed at the Chemistry Centre of the Department of Minerals and Energy

h: hyaloclastites

s: mafic schist

um: ultramafic schist

diagram for magnesium-rich rocks (Le Maitre, 1989) as shown in Figure 16.

Some of the chemical features of the Narracoota Formation volcanic rocks are well displayed in regolith materials; higher concentrations of Ni and Cr are effectively confined to areas underlain by the Narracoota Formation, whereas anomalous Pd is confined to areas underlain by the metabasaltic hyaloclastite (Subramanya et al., 1995). The latter is possibly due to the ocean-floor metamorphic characteristics of the hyaloclastite rocks.

Figures 15–18 suggest that the Narracoota metabasites have a range of compositions that could be ascribed either to the parent magma(s), or to the effects of metamorphism and ocean-floor metasomatism. The olivine-normative ultramafic rocks could represent either cumulate lithotypes in subvolcanic magma chambers, or komatiites as suggested by Hynes and Gee (1986).

Figure 19 is a tectonic discriminant diagram in which the volcanic rocks exhibit geochemical signatures ranging from ocean island to ocean ridge, with only a few data points falling within the field assigned to continental basalts. In any case, it is important to note that all data points fall well within the anorogenic fields defined for ocean-ridge or ocean-floor, ocean-island, and continental basalts (within-plate); and well outside the orogenic, or subduction-related field (plate margin). The oceanic character is confirmed by the TiO₂ versus FeO/MgO plot as shown in Figure 20. This relationship was used by Breitung and Maiden (1988) in their study of the geochemistry and tectonic environment of the Matchless metabasite belt of the Damara Orogen in Namibia. These authors found that the TiO₂ and FeO/MgO values can be used to discriminate between continental and oceanic basalts. They concluded that the Matchless metabasites were emplaced along a strike length of more than 300 km, within a tectonic environment of advanced rifting and

with the localized formation of oceanic-type sub-basins. A similar situation is envisaged for the Narracoota Formation (see **Discussion and interpretation**).

## Rare-earth elements

In the study of igneous rocks, rare-earth element (REE) patterns can be used to determine the composition of the parent melts; the extent of melting; and the modifications of the melts through mixing, differentiation, and interactions with surrounding lithologies and/or fluids.

Rare-earth element abundances for the Narracoota rocks on BRYAH are given in Table 6 and a chondrite-normalized plot is shown in Figure 21. Ultramafic schist has primitive REE abundances (2–4 times chondrite), with La/Yb_{CN} of 0.747–0.902 and distinct negative Eu anomalies (Eu/Eu* of 0.31–0.43). This suggests plagioclase fractionation, and corroborates the assumption that they may represent subvolcanic cumulates.

The metabasaltic hyaloclastite is weakly enriched in light rare-earth elements (LREE) (La/Yb_{CN} of 1.56–1.78), except for one sample (GSWA 116501; La/Yb_{CN} of 0.393). The slight positive Eu anomalies (Eu/Eu* of 1.30–1.67) indicate a lack of plagioclase fractionation. The metabasaltic hyaloclastite rocks have REE abundances of 2–10 times chondrite values, and this too highlights the essentially primitive nature of these rocks. The REE patterns for the mafic schist show two trends: one with La/Yb_{CN} of 3.39 and 2.49 (LREE enriched), and one with La/Yb_{CN} of 0.433 and 0.493 (LREE depleted). Europium anomalies of the mafic schist, although weak, are both positive and negative. It is possible these two trends relate to two different sources. The overall REE pattern displayed by the mafic schist and hyaloclastite is distinctly similar to that in MORB, such as that found in Iceland (Schilling et al., 1982).

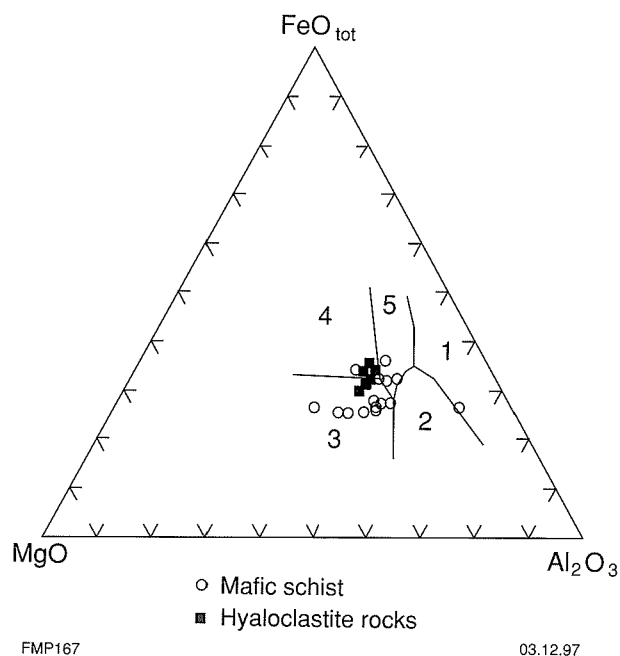


Figure 19. Tectonic discriminant diagram, after Pearce et al. (1977), illustrating the possible within-plate and anorogenic tectonic settings for the Narracoota Formation volcanic rocks. 1: Spreading-centre island; 2: orogenic; 3: ocean ridge and floor; 4: ocean island; 5: continental

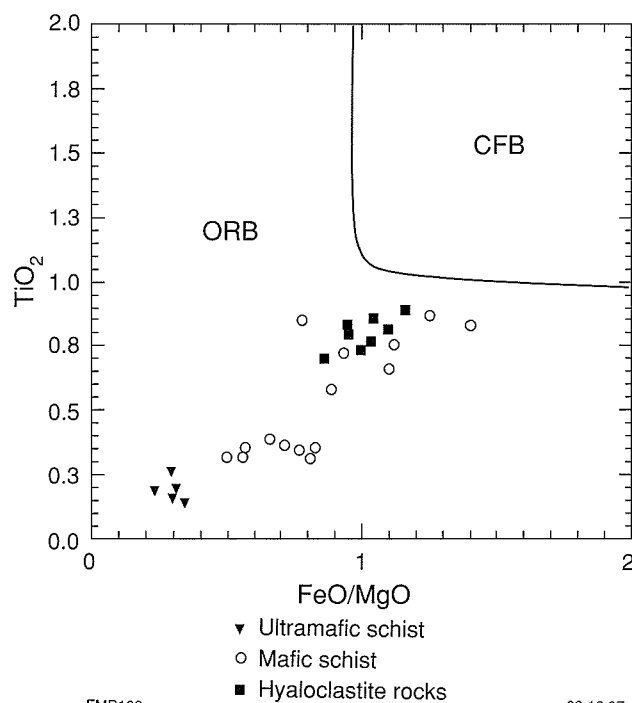


Figure 20.  $\text{TiO}_2$  versus  $\text{FeO/MgO}$  diagram showing a distinct ocean-ridge basalt (ORB) affinity of the Narracoota Formation. CFB is the field of continental flood basalts (Breitkopf and Maiden, 1988)

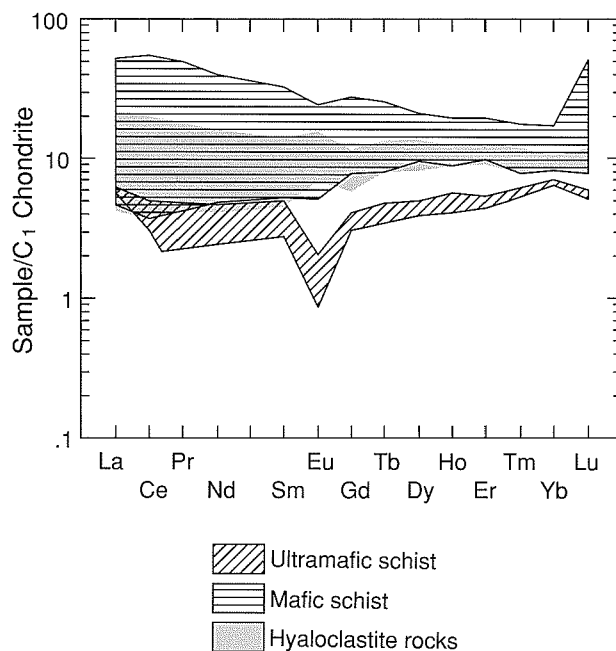
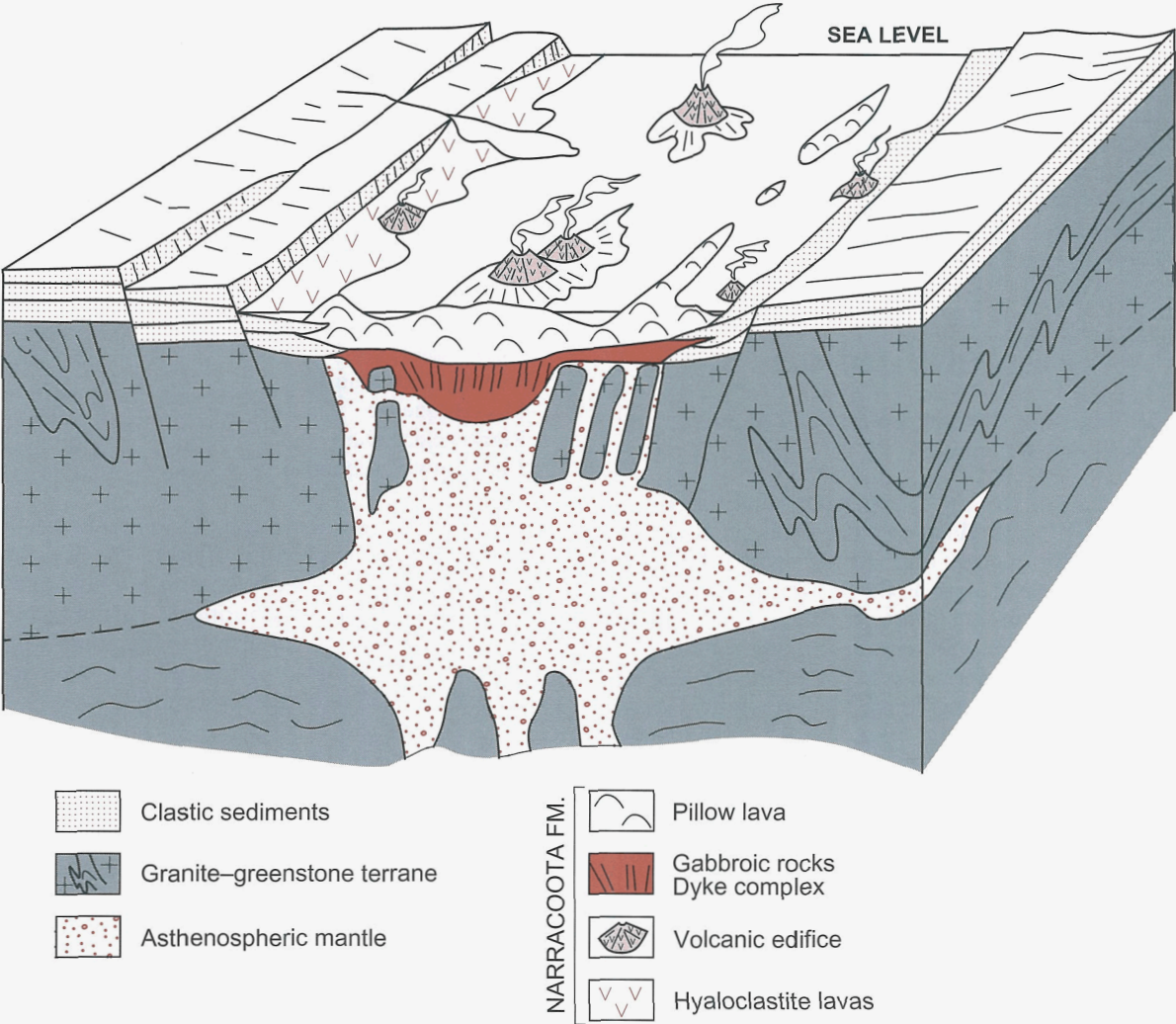


Figure 21. Chondrite-normalized REE abundances of Narracoota Formation volcanic rocks, grouped by lithotypes; normalizing views after Sun (1982)





FMP67

05.12.97

Figure 22. Model of a possible palaeoenvironmental setting of the Narracoota Formation volcanic rocks

### Discussion and interpretation

The geochemical characteristics outlined above, together with field and petrological observations, suggest that the volcanic rocks of the Narracoota Formation were derived from a depleted asthenospheric mantle source. The Narracoota igneous activity probably took place in a small oceanic basin that opened in the northern margin of the Yilgarn Craton as a result of rifting in a continental setting (Pirajno, 1996). These asthenospheric melts ascended to erupt in shallow waters (near the rifted margins) to form hyaloclastites, and in deeper waters to form pillow lavas and associated dykes and sills in a style similar to that of mid-ocean ridges. The geochemistry and petrology of the ultramafic schist suggest that it was derived from a subvolcanic olivine-cumulate precursor rock. Locally, volcanic edifices could have emerged above sea level, forming islands (volcanic ocean islands). The remnants of a volcanic island could, conceivably, be represented by the thick vent breccia intersected in BD1

south of the Murchison River. The palaeoenvironment envisaged for the Narracoota Formation volcanism is illustrated in Figure 22.

### Cainozoic geology

The Cainozoic units on BRYAH are restricted to regolith materials in sheetwash, lateritic soils, colluvium, and scree. In addition, active river and stream beds contain unconsolidated alluvial material (sand, silt, and clay — *Qa*) locally spilling into floodplains. In places, small claypans (*Qac*) are present in the Murchison River valley. Colluvium and scree are particularly well developed around the fringes of the Robinson Ranges (*Qc*). Sheetwash fans consist of colluvial sand, silts, and ferruginous clays (*Cza*). Elsewhere, Cainozoic colluvium (*Czc*) is adjacent to outcrops of the Narracoota Formation. Detailed descriptions of regolith geology and geochemistry can be found in Subramanya et al. (1995).

Lateritic duricrust and other ferruginous materials include massive ironstone (*Czli*) and related debris (*Czf*).

Calcrete (*Czk*) and silcrete (*Czz*) are not particularly well developed on BRYAH. An elongate zone of calcrete material lies 3 km north of Murphy Well at the confluence of a tributary with Millidie Creek, immediately on the west side of the Peak Hill road. Silcrete is generally associated with foliated rocks and is locally well developed over mylonites.

## Mineralization

The distribution of mineral deposits and occurrences on BRYAH is shown in Figure 23.

At the time of writing, the operating mines on BRYAH were Peak Hill and Harmony (or Baxter). Since its discovery in 1892, and up until the present day, Peak Hill remains the single largest producer of gold in the area, with a total of about 20 t (Thornett, 1995). In June 1996, Troy Resources announced the discovery of gold mineralization in the northeastern part of BRYAH, at about AMG 500660. This area is in the Marymia Inlier, within a zone of transition with the Peak Hill Schist containing amphibolite and BIF enclaves. Results of preliminary drilling are very encouraging. One drillhole intersected a gold concentration of 9.76 grams per tonne (g/t) over 15 m (announcement by Troy Resources to Australian Stock Exchange, June 1996).

Most mineral deposits (gold and copper–gold) on BRYAH are structurally controlled, of mesothermal origin, and linked with compressional tectonics and metamorphism that have affected the Bryah Group and the Peak Hill Schist. Whilst the role of compressional tectonics and metamorphism in the ore genesis processes are inferred from good empirical evidence, the precise mechanisms responsible for the mineralization remain unclear. The BRYAH lode deposits are hosted within or along the contacts of the metasedimentary and/or metavolcanic rocks. The lodes are associated with relatively narrow zones of hydrothermal alteration characterized by pyritization and alkali metasomatism.

A number of small and uneconomic manganese deposits are present. They are of supergene origin and related to manganeseiferous shale units (Horseshoe Formation).

## Gold deposits

Details of gold production from mines and prospects on BRYAH are given in Table 7. The geology of the more important gold deposits and prospects is described below.

### Peak Hill, Jubilee, and Mount Pleasant deposits

The Peak Hill, Jubilee, and Mount Pleasant deposits have been studied by Barrett (1989), who based most of his

work on drillcore samples, and Thornett (1995). These authors provided much of the information given below, augmented by data from this study.

The Peak Hill, Jubilee, and Mount Pleasant gold deposits are situated in the west-northwestern portion of the Peak Hill 'dome' structure, and are hosted in rocks of the Peak Hill Schist (Fig. 23). The mine geologists have subdivided the Peak Hill – Jubilee – Mount Pleasant lithologies into the following:

- Core sequence
- Honey quartzite
- Intermediate sequence
- Mine sequence
- Marker quartzite
- Hangingwall sequence

In the mine areas the rocks are intensely weathered to depths locally exceeding 100 m. The weathering products are predominantly kaolinitic clays and iron oxyhydroxides. This weathering is particularly well developed in zones of hydrothermal alteration, which in turn are related to high-strain zones; the latter having facilitated percolation of meteoric waters.

Hydrothermal alteration is dominated by sulfidization (pyrite) and alkali metasomatism (biotite, albite), and is contained within late-stage quartz–carbonate veins hosted in highly strained metabasites and quartz mylonites. Other important alteration minerals include iron-rich chlorite, sericite, garnet, tourmaline, dolomite, and calcite.

Current production and resources are given in Table 7. The Peak Hill mineralization is exploited in three adjoining pits, which are named from north to south: Fiveways, Peak Hill Main, and Mini pit. In plan view (Fig. 24) the entire Peak Hill mineralized system is contained within a package of mylonitic schist (Mine sequence) at the footwall of, and within, north-trending and westerly dipping shear zones. The mylonitic schist contains quartz pods, veins, lenses, and stringers, and locally graphitic quartz mylonite units (Marker quartzite; Fig. 25). The Mine sequence also contains small lenses of mafic rocks (e.g. metadolerite). Kinematic indicators (S–C surfaces) indicate a thrust movement from west to east (Thornett, 1995).

The main orebody has a westerly dip ranging from 20 to 50° (averaging 35°), and is hosted in rocks of the Mine sequence. High-grade ore zones can contain up to 15 g/t gold. The ore zones are characterized by pervasive alteration consisting of a chlorite–biotite–quartz–carbonate–graphite assemblage. The principal ore minerals are pyrite, chalcopyrite, and gold. Other ore minerals include altaite, tetrahedrite, bismuthotelluride, molybdenite, and various bismuth–lead–tellurium compounds. The gold mineralization is thought to have been deposited in at least two main stages. In the first stage, gold mineralization was deposited in the Mine sequence below, and along, the contact with the Marker quartzite. During the second stage, gold was remobilized along cross-cutting northeast-trending faults.



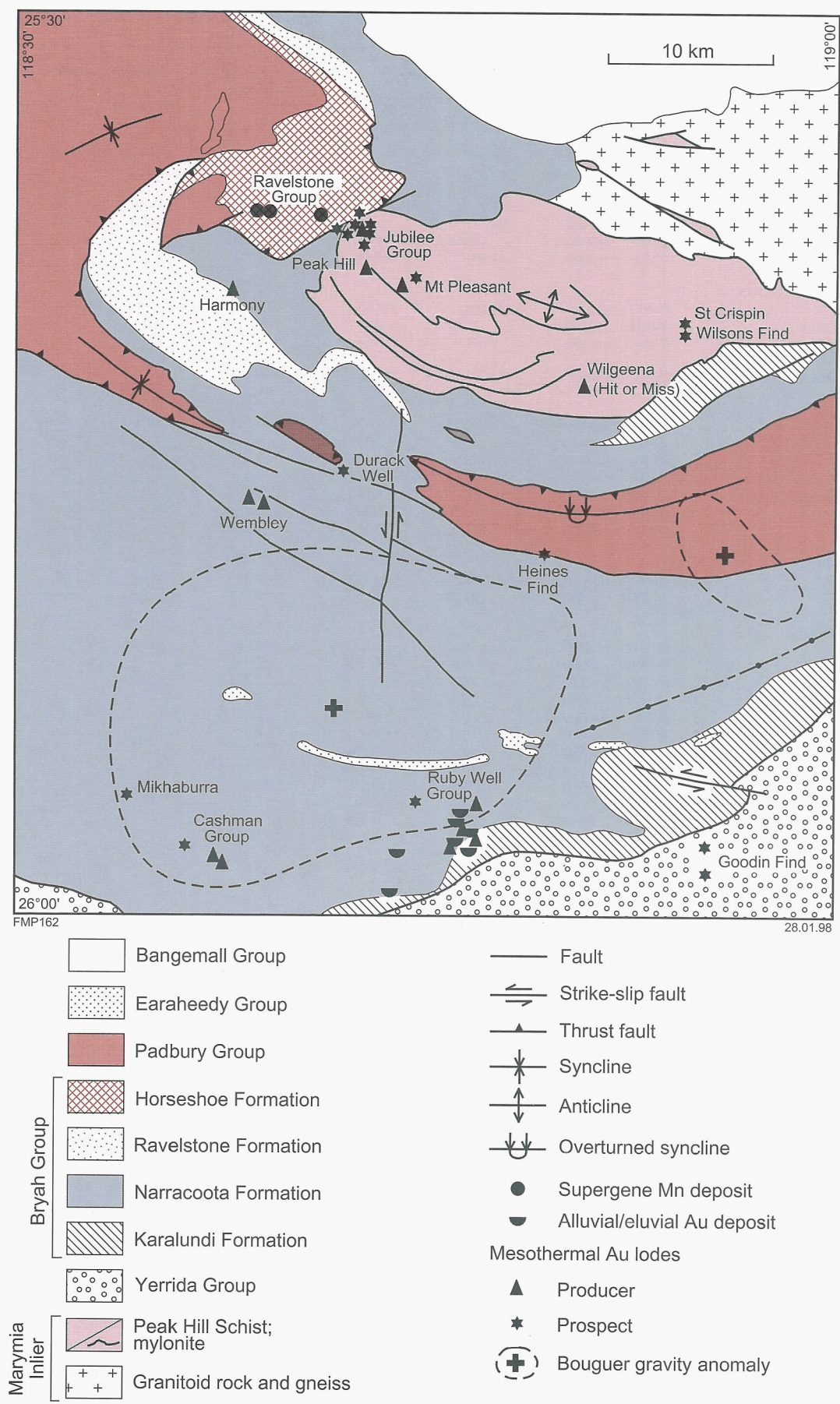


Figure 23. Simplified geology of BRYAH showing the distribution of mineral deposits and the position of Bouguer gravity anomalies



Table 7. Gold production prior to December 1995 from mines, prospects, and deposits on BRYAH

Mine/Prospect or Group (year)	AMG location		Production		Dry blowing/ alluvial	Published resources		Total
	Easting	Northing	Ore (t)	Au (kg)		Tonnes $\times 10^6$	Au (kg)	Au (kg)
Harmony	663600	7161800	307 000	1 445	0.00	2.362	7 940	9 385
PEAK HILL GROUP								
Peak Hill	673700	7163000	2 017 095	10 144.13	3.423	0.507	764	10 911.55
Five Ways	672500	7163400	302 578	—	20.332	0.391	1 617	3 016.332
Christmas Gift	670200	7163700	130.61	16.631	1.153	—	—	17.784
Morning Star	672700	7163000	17 094	44.861	14.751	—	—	59.612
MOUNT PLEASANT GROUP								
Mount Pleasant	674200	7162000	150 508	513.05	6.43	—	—	519.5
Mount Pleasant North	674100	7162300	13.77	0.043	0.0	—	—	0.043
Mount Leo	674400	7162000	642.3	3.54	0.75	—	—	4.294
WEMBLEY GROUP	659300	714800	1 791.3	31.5	1.848	—	—	33.336
JUBILEE GROUP								
Jubilee	672300	7164800	5 942.97	93.171	46.515	0.254	595	734.686
Jubilee North	671600	7165900	13.5	6.445	0.0	—	—	6.445
Blue Bell	671900	7164400	123.97	1.135	0.0	—	—	1.135
Golden Treasure Extended	672100	7165500	28.57	1.668	0.0	—	—	1.668
Oxwell, Coumbes, and Spencer	671100	7165300	859	0.316	2.3	—	—	2.6
Perseverance	670400	7165300	103.06	0.279	0.0	—	—	0.279
Reefers	671500	7166200	210	5.2	0.253	—	—	5.45
WILGEENA GROUP								
Hit or Miss	685658	7158075	13 165.3	34.112	0.0	0.600	1 464	1 498.112
Wilsons Find	691400	7158700	14.28	1.043	0.732	—	—	1.775
RUBY WELL GROUP								
Golden Hope	677500	7129400	0.0	0.0	0.765	—	—	0.765
Golden Try	677800	7129300	0.0	0.0	0.346	—	—	0.346
Lady Donna	678100	7127200	0.0	0.0	0.773	—	—	0.773
Lady Jenny	677900	7128100	0.0	0.0	0.239	—	—	0.239
Lady Margaret	677700	7128300	0.0	0.0	0.185	—	—	0.185
Stella	677700	7128600	0.0	0.0	0.392	—	—	0.392
Daisy	677600	7128900	60.2	0.598	0.997	—	—	1.595
Bloodstone (1914)	677900	7127600	40.82	0.998	0.529	—	—	1.527
Harder to Find (1911–17)	677800	7129700	7 039.8	110.677	0.0	—	—	110.677
Lucky Call (1912 and 1915)	676600	7127200	42.86	1.941	0.312	—	—	2.253
Ruby Anna (1916–17)	677200	7127800	226.53	4.785	0.0	—	—	4.785
Rubies	677500	7128900	342.0	0.517	0.233	—	—	0.750
GOLDEN GRINDSTONE (1915–17)	693800	7128100	215.31	7.139	0.0	—	—	7.139
CASHMAN GROUP	661900	7126700	8 191.37	3.39	3.867	—	—	7.168
<b>Totals</b>			<b>2 833 472.52</b>	<b>12 472.169</b>	<b>107.125</b>	<b>4.114</b>	<b>12 380</b>	<b>26 338.195</b>

The Jubilee deposit was, in 1892, first mined underground from a number of workings, the production of which is unknown. In 1992 a small pit was excavated in which a reserve of about 50 000 t was delineated with a grade of 4 g/t gold. In this pit, gold mineralization is hosted by rocks of the Hangingwall sequence, and is concentrated in a complex quartz stockwork system emplaced along the margins of a 250 m-thick undeformed metadolerite. There is gold mineralization on both the hangingwall and the footwall sides of the metadolerite body. Tourmaline is present in the ore-bearing material. Near the Jubilee pit, a north-striking and west-dipping quartz vein is almost perpendicular to the dominant foliation trend and extends for about 200 m. This vein was mined in the past and contained grades of about 30 g/t gold.

Mining at Mount Pleasant began at the turn of the century, with a production of 8000 t of ore at an average grade of 9 g/t gold. Mining resumed in the 1970s and

1980s when about 146 000 t of ore were extracted with an average grade of 3 g/t gold. The ore zones are nearly flat lying and emplaced in subparallel fashion, one above the other. The deeper northern zone is hosted by the Core sequence. Gold is hosted in quartz–carbonate veins associated with alteration zones of albite (Fig. 26), iron-rich chlorite, sericite, carbonate, and pyrite, as well as in zones of nearly flat-lying graphitic schist. The veins are either vertical, or saddle-reef type lodged in anticlinal folds.

The Core sequence is at the structural base and is well exposed in the Mount Pleasant pit, where it reaches a thickness of 55 m. The Core sequence is separated from the Intermediate sequence by the Honey quartzite — a mylonite consisting of laminated or ribbon quartz. The Core sequence rocks have a mylonitic fabric and are made up of a quartz–biotite–carbonate–muscovite(–epidote–hornblende–garnet–magnetite–pyrite) assemblage, and locally with abundant very fine zircons and monazite in

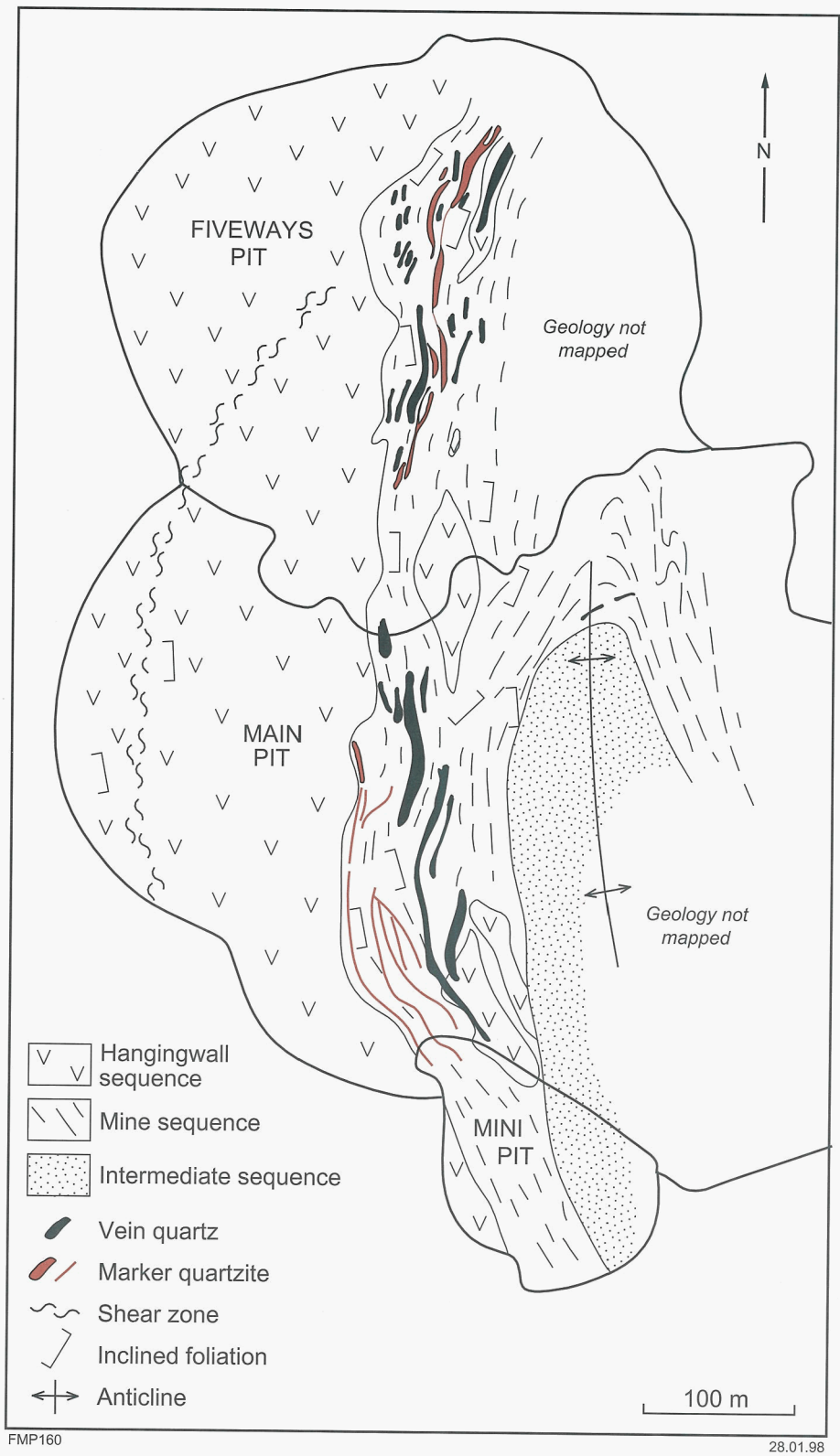
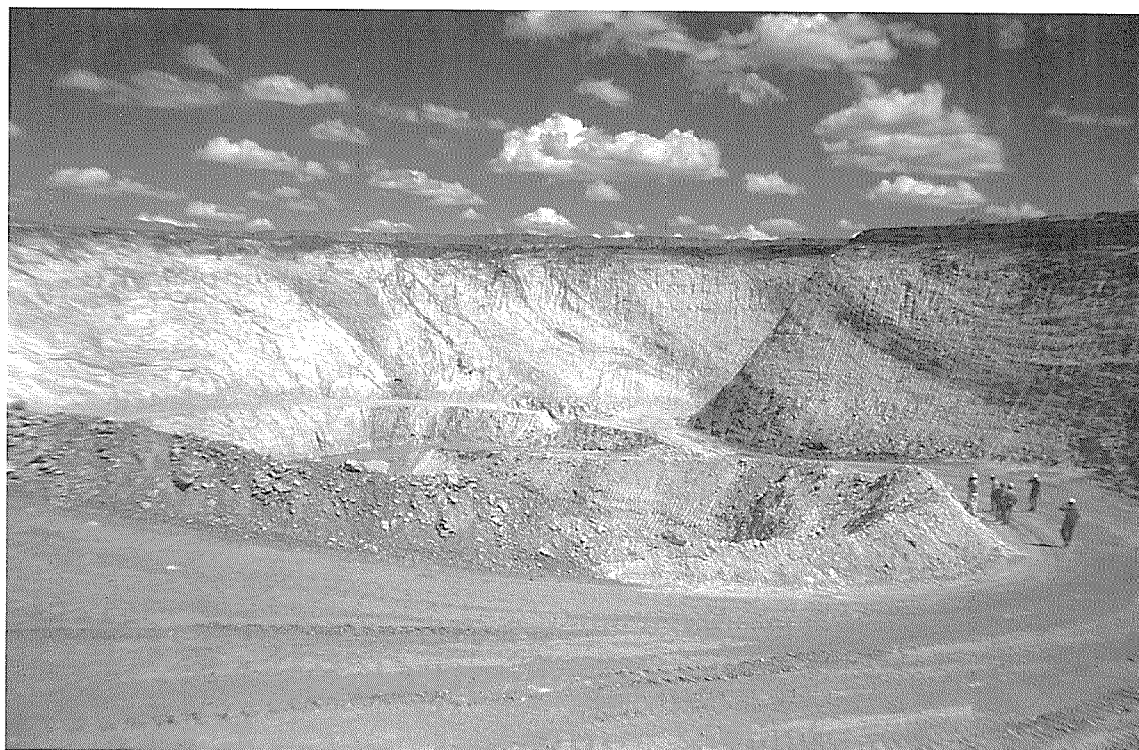


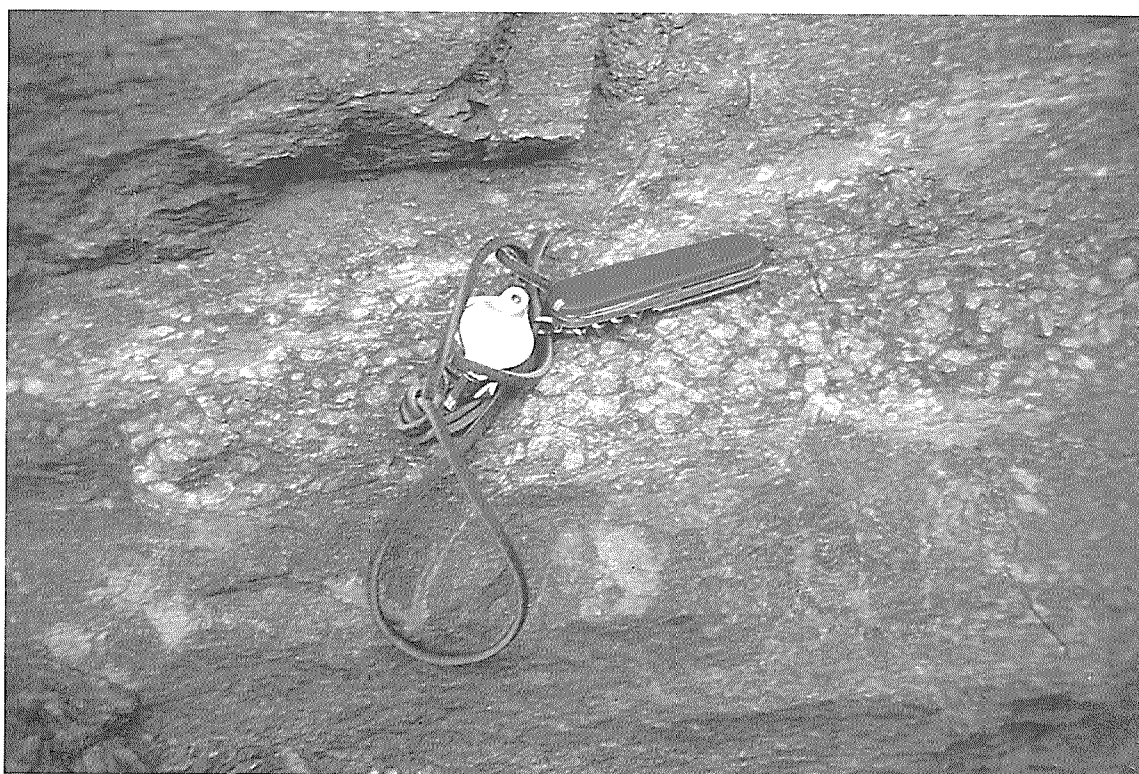
Figure 24. Sketch geological map of the Fiveways, Main, and Mini pits (Peak Hill deposit). Modified from Thornett (1995)



FMP 177

19.11.97

**Figure 25. Peak Hill Mini pit, showing the ore-bearing mylonitic schist, graphitic schist (dark bands) and Marker quartzite (unit above the upper graphitic schist)**



FMP 178

19.11.97

**Figure 26. Albite porphyroblasts in mylonitic schist at Mount Pleasant**



the biotite-rich varieties (Barrett, 1989). At Mount Pleasant, graphitic schist is present near the top and is associated with a zone of chlorite–biotite(–garnet) schist, with albite porphyroblasts (Fig. 26) containing inclusions of monazite and zircon. Geochemical discriminant plots using immobile elements suggest either a granitic (Nb, Sr, La, Ce) or a mafic–intermediate (Ni, Cr, Ti) protolith (Thornett, 1995). Barrett (1989), on the other hand, proposed that much of the Core sequence could be derived from a sedimentary protolith. The origin of the albite porphyroblasts is uncertain. Based on geochemistry, petrology, and textural features, Thornett (1995) advocates a combined hydrothermal-retrograde metamorphic origin and compares the Peak Hill – Mount Pleasant albites to those studied by Watkins (1983) in the Dalradian schists of Scotland. Another possibility that could account for the presence of the albite porphyroblasts is 'reaction softening' as proposed by Dixon and Williams (1983). These authors advanced the hypothesis, supported by geochemical and mineralogical data, that mylonitization of a quartzofeldspathic parent may be accompanied by mineralogical changes involving the breakdown of plagioclase with the release of  $\text{Na}_2\text{O}$  (and to a lesser extent  $\text{CaO}$ ) and the formation of muscovite. This would result in the production of quartz–muscovite mylonites and sodium-rich fluids.

The Intermediate sequence is discontinuous with layers up to 2 m thick, and composed of a muscovite-bearing quartz mylonite. The Intermediate sequence lies above the Honey quartzite, has an estimated thickness of between 200 and 400 m, and forms the footwall to the Mine sequence at Peak Hill and the hangingwall to the

ore zones at Mount Pleasant. The Intermediate sequence is dominantly quartz–muscovite schist with minor amounts of plagioclase, biotite, microcline, carbonate, and chlorite. This rock was interpreted by Barrett (1989) as either a felsic porphyry or an arkose. In the lower part of the Intermediate sequence, rocks are mainly biotite schist with garnet and epidote. Rocks of the Intermediate sequence exhibit millimetre-scale metamorphic differentiation layering, which define a dominant  $S_2$  schistosity (Thornett, 1995). This is interpreted by the present authors as a typical mylonitic structure.

The Mine sequence, mostly observed in drillholes, is characterized by biotite–muscovite(–chlorite–carbonate–amphibole–garnet–albite) schist and graphite schist (Figs 27 and 28). Its thickness may be in the region of 40 to 50 m. Drillcore samples of a hornblende–plagioclase–quartz rock (with garnet porphyroblasts) has been interpreted as an unaltered amphibolite (Barrett, 1989; Thornett, 1995).

The Marker quartzite is a recrystallized quartz mylonite, 1–3 m thick, which lies at the top of the Mine sequence. Outcrops of Marker quartzite exhibit radiating iron-oxide pseudomorphs after acicular crystals, and iron-oxide pseudomorphs after porphyroblasts. Windh (1992) identified the former as grunerite using Scanning Electron Microscope (SEM) analysis. The porphyroblast pseudomorphs are possibly after garnet.

The Hangingwall sequence can be up to 700 m thick and is made up of a muscovite–magnetite(–garnet–chlorite) assemblage, mafic schist, and metabasite. The

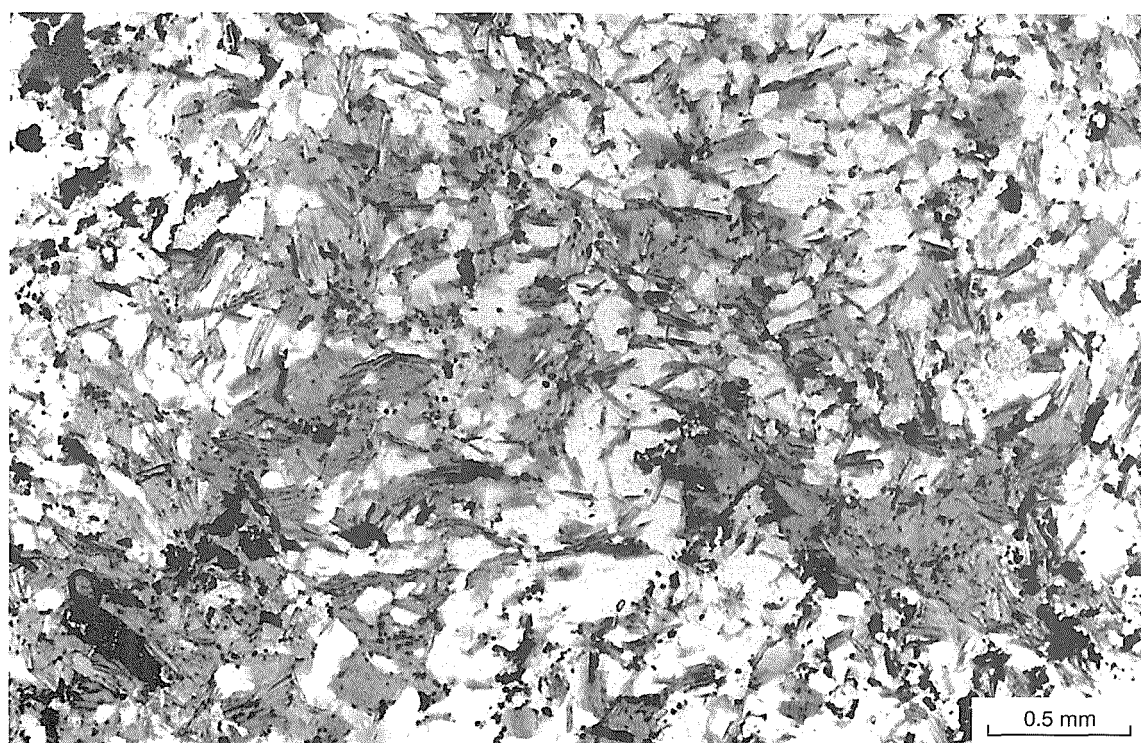


Figure 27. Photomicrograph of the Mine sequence schist showing biotite alteration; the biotite is partly retrogressed to chlorite. GSWA 119817, plane-polarized light

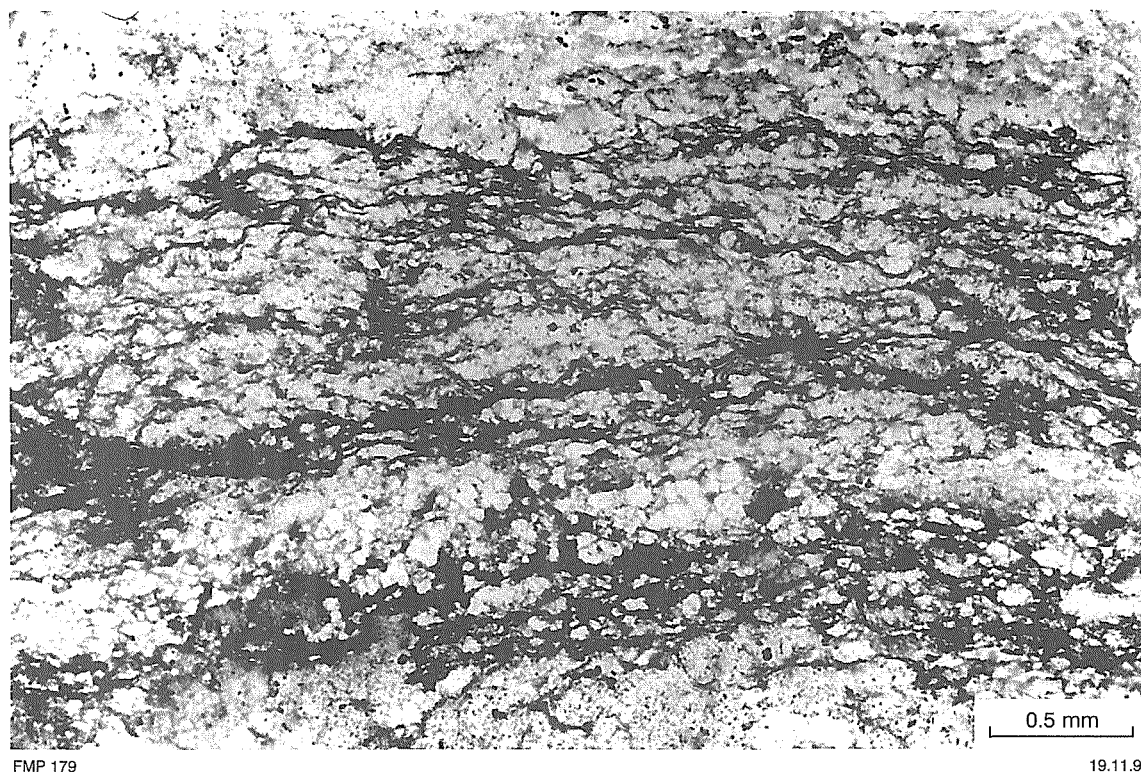


Figure 28. Photomicrograph of the Hangingwall sequence graphitic mylonite schist. GSWA 119823, plane-polarized light

metabasite is locally garnetiferous, and characterized by a metamorphic (and ?hydrothermal) assemblage containing variable amounts of hornblende, plagioclase, quartz, garnet, epidote, and titanite. The metabasite is overlain by mylonitic schist containing mainly quartz–plagioclase–biotite, locally associated with zones of albite–muscovite and garnet–epidote (calc–silicate).

### Harmony deposit

The Harmony (also known as Contact or Baxter) gold deposit is located about 10 km west of Peak Hill in a featureless area with no outcrops, which is covered by colluvium, lateritic duricrust, and hardpan material. The following brief review of the geology of the Harmony deposit can be found in Harper et al. (1998).

The Harmony gold deposit consists of a subhorizontal supergene zone hosted by ferruginous lateritic materials (transported and residual regolith); a northeast-trending, subvertical primary vein system; and carbonate-bearing breccias. Most of the ore is contained within the vein system, which is hosted in rocks of the Narracoota Formation and at the contact between the Narracoota and Ravelstone Formations (Fig. 29). The proven reserve for the Harmony deposit is 2.15 Mt, grading 3.6 g/t gold with a 1 g/t lower cutoff grade. Laterite mineralization at the time of writing has a measured resource of 259 000 t at 0.9 g/t gold, with a 0.5 g/t lower cutoff grade (Harper et al., 1998). The Harmony mineralization is hosted in a northwest-plunging antiform (Enigma structural zone) of

a southwest-dipping succession of altered mafic rocks at the top of the Narracoota Formation, and within a shear zone along the contact with the overlying metasedimentary rocks of the Ravelstone Formation. The mineralized array of quartz veins locally become closely spaced, forming a stockwork that is commonly associated with high-grade ore. Primary ore minerals include pyrite with gold inclusions, pyrrhotite, pentlandite, chalcopyrite, and scheelite. The primary mineralization was enriched by supergene processes.

Hydrothermal alteration is characterized mainly by silicification, tourmalinization, carbonitization, and locally, chloritization. Harper et al. (1998) report that mafic rocks show a paragenetic sequence of early albitization and silicification followed by muscovite and chlorite. Alteration in the metasedimentary rocks in the hangingwall is characterized mainly by sericite and chlorite. This primary alteration grades into zones of supergene alteration containing limonite, kaolinite, smectite group minerals, and hematite. The weathered bedrock extends to about 60 m in depth. Regolith studies from drillholes have revealed anomalous Au, W, As, Sb, and Se in the ferruginous materials.

### Durack prospect

The Durack prospect lies about 12 km south of Peak Hill, along and immediately west of the Old Peak Hill telegraph road. This gold deposit is covered by soil and lateritic material, and consists of primary mineralization

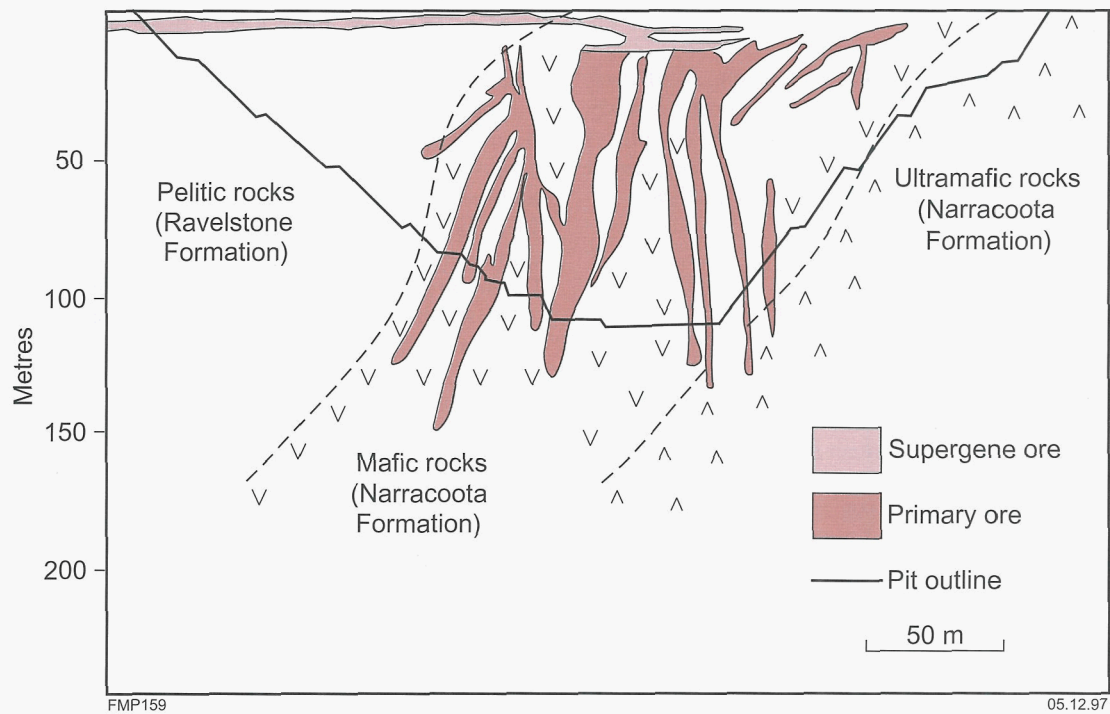


Figure 29. Diagrammatic cross section of the Harmony ore zones. Modified from Harper et al. (1998)

and a supergene mineralized zone. The prospect was identified by a soil anomaly containing up to 100 ppb gold (Nutter, A., 1997, pers. comm.).

The prospect area is underlain by an interfingering contact between the metabasite and mafic pyroclastic rocks of the Narracoota Formation and the pelitic rocks of the Ravelstone Formation. Thin, magnetite-bearing chert bands (possibly chemical sediments) are intercalated within the metabasites and define a broad synclinal structure. A number of mylonite zones, trending 120–125°, cut across the Narracoota Formation rocks and contain most of the primary mineralization. Grades intersected during drilling range from 171 to 1.8 g/t over widths of 4 to 21 m respectively (Nutter, A., 1997, pers. comm.).

The primary mineralization is contained within stockworks of thin vertical quartz veins hosted in metabasite rocks. The mineralized area is about 1.4 km long and 200 m wide. Hydrothermal alteration is pervasive and consists of quartz, chlorite, biotite, and iron-rich carbonate (ankerite). Pyrite has mineralized as fine disseminations and veinlets. Selvages of silica-pyrite-carbonate surround the mineralized zones.

The supergene mineralization at Durack is controlled by subhorizontal redox fronts within the regolith material. Zones of supergene enrichment contain grades of up to 12 g/t gold over an interval of about 5 m. In some cases the redox-front-related mineralization has developed up to 45 m each side of the primary zone. A preliminary sectional resource of 652 794 t at 2.19 g/t gold was calculated by Plutonic Operations in 1997 (Currie, D., 1997, pers. comm.).

## Wembley deposit

The Wembley deposit is about 18 km southwest of Peak Hill and 2.5 km southeast of Murphy Well (from the Peak Hill road). Although rewarding (average grade of 17.5 g/t gold), ore production was very small (less than 1800 t).

The Wembley mineralization is hosted in altered metabasite rocks within a major shear zone trending 120°. The mineralized zone has an attitude of 255/63°N. A quartz vein near the old workings has an attitude of 240/54°N. Sedimentary units are intercalated with the volcanic rocks and consist of turbiditic rocks (greywacke–shale). As at the Durack prospect, quartz mylonite units trending 120–140° are present within the metabasites.

## Hit or Miss (Wilgeena) deposit

The Hit or Miss gold mine area is 15 km southeast of Peak Hill. Production was less than 15 000 t at an average grade of 2.6 g/t gold.

The deposit lies within rocks of the Peak Hill Schist, and more specifically along the contact between the mylonites and quartz-sericite schist. A northerly trending, east-dipping, stoped-out ore lens was about 2 m thick. The mineralization is hosted in quartz-muscovite-magnetite schist. Grab samples from the old excavations returned values ranging from 3 to 14 g/t gold (Mountford, 1984). At a later stage, mineable reserves were delineated giving a total of about 600 000 t at 2.44 g/t gold (Whitfield, 1987).

## St Crispin prospect

The St Crispin prospect is 20 km east-southeast of Peak Hill. The mineralization lies along a north-northwesterly trending structure and is hosted in sericite(–graphite) schist of the Peak Hill Schist. Quartz veins are present in the schist rocks and may host the mineralization.

## Heines Find prospect

The Heines Find prospect is 20 km south-southeast of Peak Hill. Mineralization can be traced for about 6 km along the easterly trending contact between rocks of the Narracoota Formation and the Heines Member of the Wilthorpe Formation. This contact has a dip of 80°N and is sheared. In this area the Narracoota Formation consists of strongly deformed pillow lavas and chlorite schist. The overlying Heines Member sedimentary rocks include a basal polymictic conglomerate.

## Goodin Find prospect

The Goodin Find gold prospect is about 80 km north of Meekatharra, near the Great Northern Highway. The mineralization is close to the Goodin Fault, which marks the northwestern boundary of the Doolgunna Formation.

## Ruby Well Group

The Ruby Well area includes a number of mineral leases from which gold has been produced either from surface materials or from hard rock. The Ruby Well leases lie on the north side of the Great Northern Highway, about 80 km from Meekatharra and 4–5 km east of the Peak Hill road turn-off.

The area is underlain by the Narracoota, Doolgunna, and Karalundi Formations. The Hard to Find, Ruby Anne, and Lucky Call deposits lie within the mafic schist of the Narracoota Formation, and were exploited between 1912 and 1917. Most of the current production (figures not available) comes from a number of dry-blowing workings surrounding these old mines.

## Cashman deposit

The Cashman area includes a number of small mineral occurrences and deposits, which contain copper and copper–gold. The old Cashman copper mine

(AMG 621270) is about 250 m from the gold workings. In 1917 this mine produced about 7 t of copper ore, grading 16.5% copper (Marston, 1979). The copper mineralization consists of a metre-wide cupriferous limonite vein striking 222°, with a shallow dip to the northwest. Ore minerals are chrysocolla and malachite, and form as disseminations and veinlets (Marston, 1979). In 1937 there was a small production of gold ore from quartz veins. In 1986–87 the gold potential of the Cashman area was reassessed, and on the basis of this work a small openpit was excavated from which 8000 t of ore material was produced and stockpiled (Whitfield, 1987). Gold mineralization is hosted in quartz veins within metabasaltic hyaloclastite. A quartz vein 0.1 m thick, in the pit, has an attitude of 295/35°N; while at, and near, the surface, supergene enrichment is present in a horizon about 30 m wide and dipping 20°N (Whitfield, 1987).

## Mikhaburra deposit

The old Mikhaburra gold mine (also known as Holdens Find) lies in volcanic rocks of the Narracoota Formation, in the southwestern part of BRYAH (AMG 563307). The recorded production of the Mikhaburra mine totals about 226 kg (McLeod, 1970). The mineralization is associated with a system of auriferous quartz veins emplaced along a shear zone trending about 130–150° and dipping 68°S. The volcanic rocks include mainly chlorite schist. A quartz vein with an attitude of 120/58°S lies to the west of the old workings. This vein is about 1 m wide and locally displays a laminated structure.

## Manganese deposits

Manganese mineralization on BRYAH lies about 5 km northwest of the Peak Hill gold mine (Ravelstone; Table 8). This mineralization is part of a manganese field, which comprises deposits in the Mount Fraser (PADBURY) and Horseshoe (JAMINDI) areas. The manganese mineralization is of supergene origin and is related to manganese-rich shale units of the Horseshoe Formation. This supergene enrichment appears to have a structural control along an easterly trending shear zone. The ore is lateritic, locally pisolitic in nature, and forms caps that overlie the primary manganese-rich sedimentary material. The chief ore mineral is pyrolusite.

In the Ravelstone area, mining took place sporadically between 1922 and 1960 with a production of about 110 000 t of manganese ore coming from three leases.

Table 8. Copper and manganese production prior to December 1995 on BRYAH

Mine/prospect	Metal	AMG location		Production		Published resources		
		Easting	Northing	Ore/concentrate (t)	Metal (kg)	Tonnes	Metal (kg)	Total metal (kg)
Cashman	Cu	662129	7126994	7	1	—	—	1
Ravelstone Group	Mn	669000	7167500	2 254	1 546	237 000	109 000	110 546



The manganese orebodies strike approximately east, and may reach lengths of up to 100 m with widths of up to 30 m. A resource estimate from one ore zone is 4000 t at 40% manganese (de la Hunty, 1963).

## Discussion and interpreted ore genesis for the gold lode mineralization

Most of the known epigenetic gold mineralization is within the deformed and metamorphosed (greenschist facies) rocks of the Peak Hill Schist and the Bryah and Padbury Groups. The lode deposits are generally hosted in metasedimentary and/or metavolcanic rocks, or along their contact zones. The lodes are spatially associated with high-strain zones and hydrothermal alteration dominated by pyrite, quartz–muscovite, biotite, and alkali feldspars. The mineralization is contained in both ductile and brittle-ductile shears (e.g. Peak Hill deposit) and in discrete brittle fractures (e.g. Cashman deposit), indicating a relationship between the structural style and the rheology of the host rocks. The development of ductile, brittle-ductile, and brittle structures (zones of high permeability) was accompanied by the infiltration of hydrothermal fluids, which produced alteration and mineralization.

The precise timing of the mineralization is difficult to ascertain. Windh (1992) suggested syn- $D_3$ , but from field and petrological observations it is more likely that circulation of mineralizing fluids took place during a continuum related to  $D_1$ – $D_2$  tectonism and metamorphism under conditions of ductile or brittle-ductile regimes, with perhaps some remobilization into brittle structures occurring during  $D_3$ .

The nature of the mineralizing fluids is poorly understood. Alteration assemblages at Peak Hill and Mount Pleasant indicate that the ore fluids were enriched in Fe, K, Na, S, B,  $\text{CO}_2$ ,  $\text{SiO}_2$ , and  $\text{H}_2\text{O}$  (Thornett, 1995). Fluid inclusion studies of mineralized materials from the Fortnum and Labouchere gold deposits on MILGUN (Dyer, 1991; Windh, 1992) indicate that the ore fluids were  $\text{H}_2\text{O}$ - and  $\text{H}_2\text{O}$ – $\text{CO}_2$ -rich, with salinities of 7–12 wt% and 5–17 wt% NaCl equivalent respectively. Microthermometric measurements (Dyer, 1991; Windh, 1992) gave temperatures ranging from about 170 to 320°C. Dyer (1991) concluded that the hydrothermal mineralization in the Labouchere–Fortnum area was generated by the mixing of two fluids of different density and salinity: deeply sourced, hot, saline,  $\text{CO}_2$ -bearing fluids mixed with cooler, less saline, near-surface aqueous fluids.

Lead-isotope data suggest that mineralization occurred between 1.92 and 1.7 Ga (Windh, 1992; Thornett, 1995). The results of lead isotopic studies also indicate that the lead was derived from Yilgarn Craton rocks (Dyer, 1991; Windh, 1992; Thornett, 1995). There is also a suggestion that the lead from the Peak Hill deposit (in the Peak Hill Schist, on the southwestern tip of the Marymia Inlier — see Fig. 1) is similar to the lead obtained from a sample of galena in the Marymia deposit (McMillan, 1993).

Hydrothermal solutions responsible for the emplacement of mesothermal lodes are generated in tectonically active regions, and are associated with compressional and extensional tectonics (Kerrick and Cassidy, 1994). The mesothermal-style lodes of the Peak Hill Schist and the Bryah and Padbury Groups were formed in a compressional setting characterized by thin-skinned thrusting associated with retrograde mineral assemblages (Occhipinti et al., 1996; Pirajno et al., 1996; Pirajno, 1996). From work carried out elsewhere (e.g. Fortnum and Labouchere gold deposits) it is possible to infer that, in general, the fluids were  $\text{CO}_2$ -bearing, with a salinity of around 10% NaCl equivalent and temperatures of about 300°C (Dyer, 1991; Windh, 1992). Available evidence indicates that the mineralizing fluids were at first generated during compression and dehydration, and later moved along ductile and brittle structures. During extension, meteoric fluids would have infiltrated along the same structures and mixed with the hotter metamorphic solutions. The whole mechanism could be repeated again in the next phase of compression and extension, leading to multiphase ore genesis processes in which the latest phase leaves the most detectable imprint.

## Aeromagnetic and gravity data

Aeromagnetic and gravity data were used in the geological, tectonic, and structural interpretation of BRYAH.

The total-magnetic-intensity (TMI) image of BRYAH is shown in Figure 30. This is the result of an aeromagnetic survey flown by Tesla Airborne Geoscience between July and October 1994 over PEAK HILL and GLENGARRY (1:250 000) and the northeastern part of ROBINSON RANGE. A Scintrex (model H8) cesium-vapour magnetometer was used. Flight lines were oriented north–south and northwest–southeast, depending on the regional structural grain, with a spacing of 400 m and nominal terrain clearance of 60 m. Image processing was performed using ERMMapper software.

The most striking features are the curved, continuous and narrow, very high amplitude magnetic anomalies, which correspond to outcrops of BIF (Robinson Range and Horseshoe Formations). Equally striking is a domain of very low magnetization in the southeastern corner of the map sheet, which corresponds to outcrops of the Doolgunna Formation (Yerrida Group). The tectonic contact between the Bryah Group and the Doolgunna Formation is marked by a discontinuous sinuous band of highly magnetized materials, which probably correspond to outcrops of the Karalundi Formation. These short, equidimensional magnetic elements of the Karalundi Formation may be due to titanomagnetite concentrations along the foresets of cross-bedded quartz arenite units. Other domains of low magnetization include areas underlain by rift-fill facies metasedimentary rocks of the Ravelstone Formation, and possibly metasedimentary rocks intercalated with volcanic rocks of the Narracoota Formation. The Peak Hill Schist is also

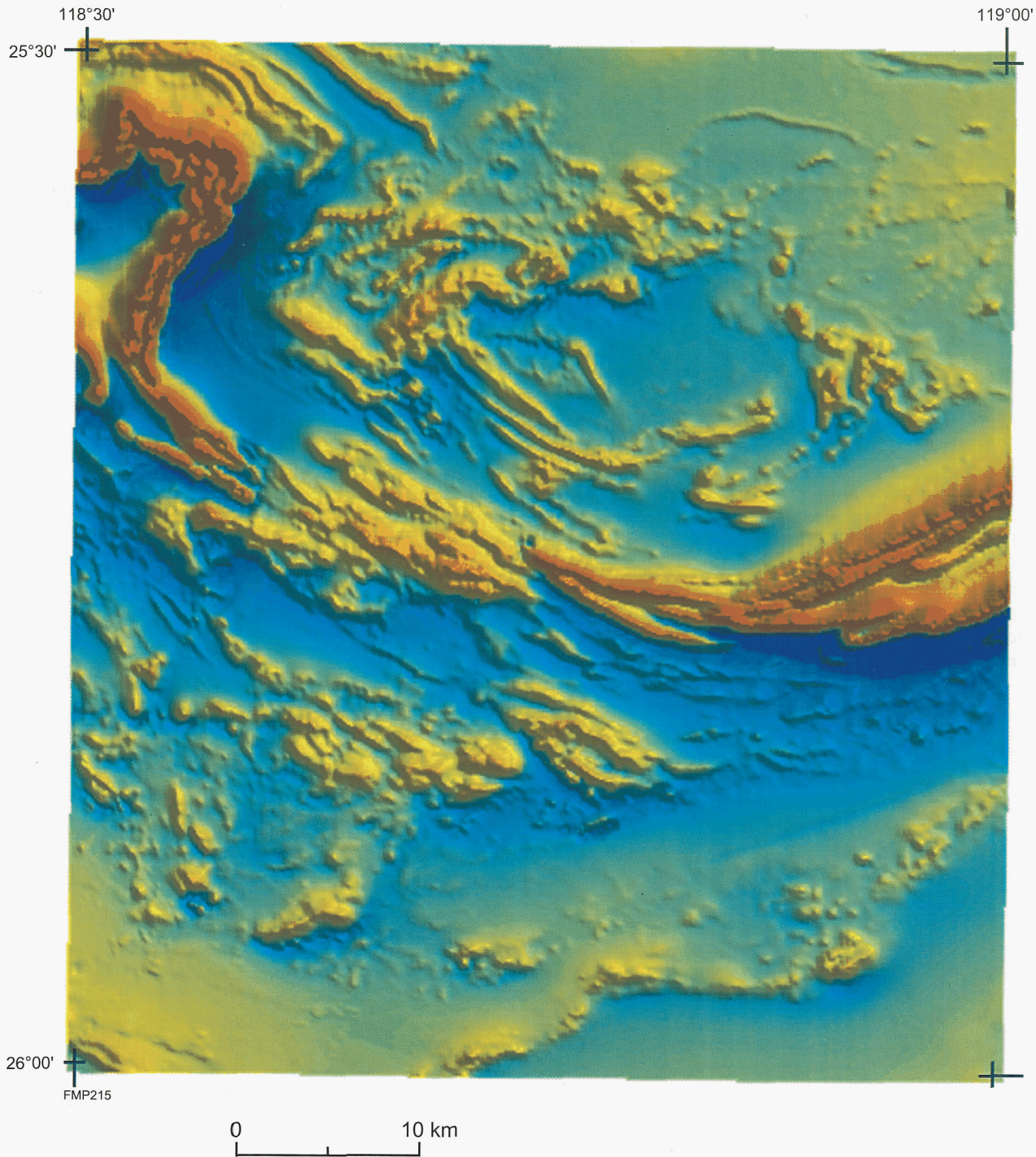


**Figure 30. Aeromagnetic image of BRYAH. Data is from the Department of Minerals and Energy, Glengarry airborne geophysical survey**

characterized by very low magnetic intensity, with the exception of high-amplitude, thin magnetic elements arranged in linear belts. These probably correspond to blastomylonites containing disseminated magnetite porphyroblasts. The metabasites of the Narracoota Formation show variable magnetic signatures, ranging from very weakly to highly magnetized domains. The latter are lens shaped, following the trend of the regional  $D_2$  foliation, with the exception of a well-defined

magnetic high in the southwestern part of BRYAH, which has an east-northeasterly trend. As mentioned previously, drilling into this magnetic anomaly has intersected 520 m of vent-breccia material. It is of considerable interest that this volcanic breccia and the associated magnetic anomaly coincide with a positive Bouguer gravity anomaly. In the northern part of BRYAH, magnetic patterns become more subdued as the cover of the Bangemall Group rocks increase in thickness. Archaean granite and

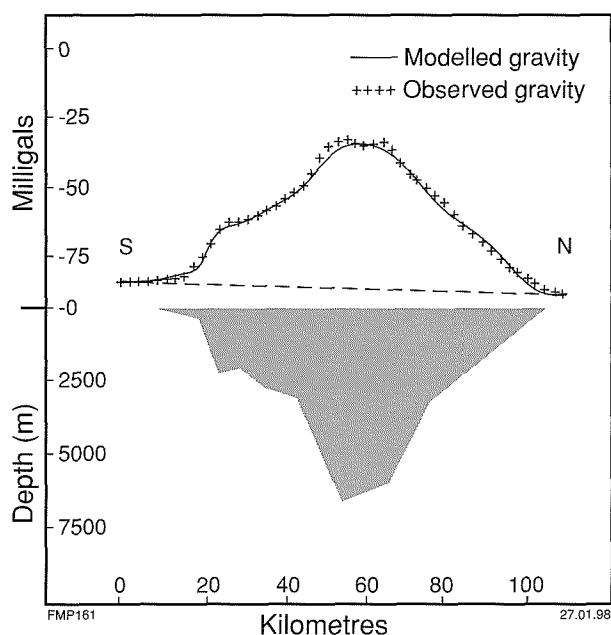


**Figure 31.** Gravity model of the north-south section shown in Figure 1, obtained assuming a background density of  $2.67 \text{ g/cm}^3$ . Modelling was carried out by Mr S. Shevchenko (GSWA). The section shows the depth and extent of the Narracoota Formation rocks modelled in terms of the observed gravity data. Gravity data come from the AGSO database

gneiss have low to medium responses with predominantly easterly orientations.

A gravity map of PEAK HILL and GLENGARRY (1:250 000), and part of ROBINSON RANGE and WILUNA (1:250 000), was obtained from the AGSO database (also available at the web site <http://www.ned.dem.csiro.au/AGCR/4dgm/grasslinks>). A regional positive gravity anomaly underlies the central and southern parts of BRYAH. As noted previously, the largest gravity anomaly within the regional high is in the southwest, and is coincident with an elliptically shaped aeromagnetic

anomaly and a thick sequence of volcanic breccia material. The gravity contours reflect either a high-density basement feature or a thick pile of high-density basic rocks. The BRYAH gravity anomaly was modelled assuming a background density of  $2.67 \text{ g/cm}^3$ . In this model the gravity anomaly can be explained by a body of mafic rocks (Narracoota Formation) about 7 km deep, as shown in Figure 31.

Positive gravity anomalies commonly characterize intracontinental rift zones. Gravity data of rift zones show that large positive Bouguer anomalies underlie many rift structures (e.g. Mid-Continent Rift; Hutchinson et al., 1990). Modelling of these positive gravity anomalies suggest that rifts are underlain by large volumes of mafic igneous material. Geological evidence further indicates that this igneous material is likely to consist of great thicknesses of mafic lavas. However, it seems that the lavas alone, in many cases, cannot account for the magnitude of the gravity anomaly. Therefore, it is widely agreed that large positive gravity anomalies in rift structures can only be explained by the underplating of a large high-density body in the lower crust (Hutchinson et al., 1990).

## Acknowledgements

We wish to acknowledge the cooperation of, and discussions with, the staff at the Peak Hill and Harmony mines; particularly Sue Thornett who generously shared her knowledge with us. We also wish to acknowledge North Exploration who provided access to, and material from, the core of diamond drillhole BD1.



## References

- ADAMIDES, N. G., 1995, Doolgunna, W.A. Sheet 2646: Western Australia Geological Survey, 1:100 000 Geological Series.
- BARNETT, J. C., 1975, Some probable Lower Proterozoic sediments in the Mount Padbury area: Western Australia Geological Survey, Annual Report 1974, p. 52–54.
- BARRETT, F., 1989, A study of wallrock alteration associated with gold mineralization — Peak Hill and Mount Pleasant area: Geopeko Ltd, Report 89/36P (unpublished).
- BATES, R. L., and JACKSON, J. A., (editors), 1987, Glossary of geology, 3rd edition: Alexandria, Virginia, American Geological Institute, 788p.
- BREITKOPF, J. H., and MAIDEN, K. J., 1988, Tectonic setting of the Matchless Belt pyritic copper deposits, Namibia: *Economic Geology*, v. 83, p. 710–723.
- BUNTING, J. A., 1986, Geology of the eastern part of the Nabberu Basin, Western Australia: Western Australia Geological Survey, Bulletin 131, 130p.
- BUTCHER, K., and FREY, M., 1994, Petrogenesis of metamorphic rocks: New York, Springer-Verlag, 318p.
- de HAVELLAND, D. W., 1985, Gold and ghosts (a prospector's guide to metal detecting and history of the Australian Goldfields) — volume 1: Perth, Western Australia, Hesperian Press, 325p.
- de HAVELLAND, D. W., 1986, Gold and ghosts (a prospector's guide to metal detecting and history of the Australian Goldfields) — volume 2: Perth, Western Australia, Hesperian Press, 382p.
- de la HUNTY, L. E., 1963, The geology of the manganese deposits of Western Australia: Western Australia Geological Survey, Bulletin 116, 122p.
- DIXON, J., and WILLIAMS, G., 1983, Reaction softening in mylonites from the Arnaboll Thrust, Sutherland: *Scottish Journal of Geology*, v. 19, p. 157–168.
- DYER, F. L., 1991, The nature and origin of gold mineralization at the Fortnum, Nathans and Labouchere deposits, Glengarry Basin, Western Australia: University of Western Australia, Honours thesis (unpublished).
- FISCHER, R. V., and SCHMINCKE, H.-U., 1984, *Pyroclastic Rocks*: Berlin, Springer-Verlag, 472p.
- GEE, R. D., 1979, The geology of the Peak Hill area: Western Australia Geological Survey, Annual Report 1978, p. 55–62.
- GEE, R. D., 1987, Peak Hill, W.A. (2nd edition): Western Australia Geological Survey, 1:250 000 Geological Series Explanatory Notes, 23p.
- GEE, R. D., 1990, Nabberu Basin, in *Geology and mineral resources of Western Australia*: Western Australia Geological Survey, Memoir 3, p. 202–210.
- GEE, R. D., and GREY, K., 1993, Proterozoic rocks on the Glengarry 1:250 000 sheet — stratigraphy, structure and stromatolite biostratigraphy: Western Australia Geological Survey, Report 41, 30p.
- GREY, K., 1994, Stromatolites from the Palaeoproterozoic Earahedy Group, Earahedy Basin, Western Australia: *Alcheringa*, v. 18, p. 187–218.
- HARPER, M. A., HILLS, M. G., RENTON, J. I., and THORNETT, S. E., 1998, Gold deposits of the Peak Hill area, in *Geology of Australian and Papua New Guinean mineral deposits*: Australasian Institute of Mining and Metallurgy, Monograph 22, p. 81–88.
- HEYDON, O. A. M., 1991, Gold at Peak Hill: Perth, Western Australia, Hesperian Press, 301p.
- HUGHES, C. J., 1982, *Igneous petrology*: Amsterdam, Elsevier, 551p.
- HUTCHINSON, D. R., WHITE, R. S., CANNON, W. F., and SCHULZ, K. J., 1990, Keweenaw Hot Spot — geophysical evidence for a 1.1 Ga mantle plume beneath the midcontinent rift system: *Journal of Geophysical Research*, v. 95, p. 19869–19884.
- HYNES, A., and GEE, R. D., 1986, Geological setting and petrochemistry of the Narracoota Volcanics, Capricorn Orogen, Western Australia: *Precambrian Research*, v. 31, p. 107–132.
- IRVINE, T. N., and BARAGAR, W. R. A., 1971, A guide to the chemical composition of the common volcanic rocks: *Canadian Journal of Earth Sciences*, v. 8, p. 523–548.
- JENSEN, L. S., 1976, A new cation plot for classifying subalkalic volcanic rocks: Ontario Division of Mines, Miscellaneous Paper, no. 66, 22p.
- KERRICH, R., and CASSIDY, K. F., 1994, Temporal relationships of lode gold mineralization to accretion, magmatism, metamorphism and deformation — Archean to present, a review: *Ore Geology Reviews*, v. 9, p. 263–310.
- LE MAITRE, R. W., 1989, *A classification of igneous rocks and glossary of terms*: Oxford, Blackwell Scientific Publications, 193p.
- LISTER, G. S., and SNOKE, A. W., 1984, S–C mylonites: *Journal of Structural Geology*, v. 6, p. 617–638.
- MacLEOD, W. N., 1970, Peak Hill, W.A.: Western Australia Geological Survey, 1:250 000 Geological Series Explanatory Notes, 21p.
- McDONALD, I. R., 1994, Final Report on the Glengarry Nickel project E52/502 and E51/384: Western Australia Geological Survey, M-series, Item 7706 (unpublished).
- McMILLAN, N. H., 1993, Dome, in *Kalgoorlie 93 — an international conference on crustal evolution, metallogeny and exploration of the Eastern Goldfields compiled by P. R. WILLIAMS and J. A. HALDANE*: Australian Geological Survey Organisation, Extended Abstracts, p. 243–244.
- McPHIE, J., DOYLE, M., and ALLEN, R., 1993, *Volcanic textures*: Hobart, Tasmania, Tasmanian Government Printing Office, 198p.
- MARSTON, R. J., 1979, Copper mineralization in Western Australia: Western Australia Geological Survey, Bulletin 13, 208p.
- MARTIN, D. McB., 1994, Stratigraphy and sedimentology of the Early Proterozoic Labouchere Formation, Padbury Group — constraints on the tectonic setting of the northern Yilgarn Craton: University of Western Australia, PhD thesis (unpublished).
- MARTIN, D. McB., in prep., Stratigraphy and structure of the Palaeoproterozoic Padbury Group, Milgun 1:100 000 sheet, Western Australia: Western Australia Geological Survey, Report 62.
- MOUNTFORD, B. R., 1984, Preliminary geological report on Prospecting Licences P52/104 and P52/105, Mount Padbury area, Western Australia: Western Australia Geological Survey, M-series, Item 3688 (unpublished).



- MUHLING, P. C., and BRAKEL, A. T., 1985, Geology of the Bangemall Group — the evolution of an intracratonic Proterozoic basin: Western Australia Geological Survey, Bulletin 128, 265p.
- MYERS, J. S., 1990, Precambrian tectonic evolution of part of Gondwana, southwestern Australia: *Geology*, v. 18, p. 537–540.
- MYERS, J. S., 1993, Precambrian history of the West Australian craton and adjacent orogens: *Annual Review of Earth and Planetary Science*, v. 21, p. 453–485.
- MYERS, J. S., SHAW, R. D., and TYLER, I. M., 1996, Tectonic evolution of Proterozoic Australia: *Tectonics*, v. 15, p. 1431–1446.
- NELSON, D. R., 1995, Compilation of SHRIMP U–Pb zircon geochronology data, 1994: Western Australia Geological Survey, Record 1995/3, 244p.
- NELSON, D. R., 1996, Compilation of SHRIMP U–Pb zircon geochronology data, 1995: Western Australia Geological Survey, Record 1996/5, 168p.
- OCCHIPINTI, S. A., GREY, K., PIRAJNO, F., ADAMIDES, N. G., BAGAS, L., DAWES, P., and LE BLANC SMITH, G., 1997a, Stratigraphic revision of Palaeoproterozoic rocks of the Yerrida, Bryah and Padbury Basins (former Glengarry Basin): Western Australia Geological Survey, Record 1997/3, 57p.
- OCCHIPINTI, S. A., SWAGER, C. P., and MYERS, J. S., 1997b, Padbury, W.A. Sheet 2546: Western Australia Geological Survey, 1:100 000 Geological Series.
- OCCHIPINTI, S. A., SWAGER, C. P., and PIRAJNO, F., 1996, Structural and stratigraphic relationships of the Padbury Group, Western Australia — implications for tectonic history: Western Australia Geological Survey, *Annual Review* 1995–96, p. 88–95.
- PASSCHIER, C. W., and TROUW, R. A. J., 1996, *Micro-tectonics*: Heidelberg, Springer-Verlag, 289p.
- PEARCE, T. H., GORMAN, B. E., and BIRKETT, T. C., 1977, The relationship between major element chemistry and tectonic environment of basic and intermediate volcanic rocks: *Earth and Planetary Science Letters*, v. 36, p. 121–132.
- PETERS, S. G., 1993, Polygenetic mélange in the Hodgkinson goldfield, Northern Tasman Orogenic Zone: *Australian Journal of Earth Sciences*, v. 40, p. 115–129.
- PIRAJNO, F., 1996, Models for the geodynamic evolution of the Palaeoproterozoic Glengarry Basin, Western Australia: Western Australia Geological Survey, *Annual Review* 1995–96, p. 96–103.
- PIRAJNO, F., and ADAMIDES, N. G., 1997, Thaduna, W.A. Sheet 2846: Western Australia Geological Survey, 1:100 000 Geological Series.
- PIRAJNO, F., ADAMIDES, N. G., and FERDINANDO, D., 1997, Glengarry, W.A. Sheet 2645: Western Australia Geological Survey, 1:100 000 Geological Series.
- PIRAJNO, F., ADAMIDES, N. G., OCCHIPINTI, S. A., SWAGER, C. P., and BAGAS, L., 1995a, Geology and tectonic evolution of the early Proterozoic Glengarry Basin, Western Australia: Western Australia Geological Survey, *Annual Review* 1994–95, p. 71–80.
- PIRAJNO, F., BAGAS, L., SWAGER, C. P., OCCHIPINTI, S. A., and ADAMIDES, N. G., 1996, A reappraisal of the stratigraphy of the Glengarry Basin, Western Australia: Western Australia Geological Survey, *Annual Review* 1995–96, p. 81–87.
- PIRAJNO, F., and OCCHIPINTI, S. A., 1995, Base metal potential of the Paleoproterozoic Glengarry and Bryah Basins, Western Australia — recent developments in base metal geology and exploration: *Australian Institute of Geoscientists, Bulletin* 16, p. 51–56.
- PIRAJNO, F., OCCHIPINTI, S. A., LE BLANC SMITH, G., and ADAMIDES, N., 1995b, Pillow lavas in the Peak Hill terranes: Western Australia Geological Survey, *Annual Review* 1993–94, p. 63–66.
- RAYMOND, L. A., 1984a, Classification of mélanges: Geological Society of America, Special Paper 198, p. 7–20.
- RAYMOND, L. A., 1984b, (editor), Mélanges, their nature, origin and significance: Geological Society of America, Special Paper 198, 170p.
- RUSSELL, J., GREY, K., WHITEHOUSE, M., and MOORBATH, S., 1994, Direct Pb/Pb age determination of Proterozoic stromatolites from the Ashburton and Nabberu Basins, Western Australia: 8th International Conference on Geochemistry, Geochronology and Cosmochronology, Berkeley, USA, June 1994, Abstracts, p. 8.
- SCHILLING, J.-G., MEYER, P. S., and KINGLSEY, R. H., 1982, Evolution of the Iceland hot spot: *Nature*, v. 296, p. 313–320.
- STANTON, R. L., 1989, The precursor principle and the possible significance of stratiform ores and related chemical sediments in the elucidation of processes of regional metamorphic formation: *Philosophical Transactions of the Royal Society of London*, v. A328, p. 529–646.
- SUBRAMANYA, A. G., FAULKNER, J. A., SANDERS, A. J., and GOZZARD, J. R., 1995, Geochemical mapping of the Peak Hill 1:250 000 sheet: Western Australia Geological Survey, Explanatory Notes, 59p.
- SUN, S.-S., 1982, Chemical composition and origin of the Earth's primitive mantle: *Geochimica et Cosmochimica Acta*, v. 46, p. 179–192.
- SWAGER, C. P., and MYERS, J. S., 1997, Milgun, W.A. Sheet 2547: Western Australia Geological Survey, 1:100 000 Geological Series.
- THORNETT, S., 1995, The nature and timing of gold mineralization in the Proterozoic rocks of the Peak Hill district: University of Western Australia, MSc thesis (unpublished).
- TYLER, I. M., and THORNE, A. M., 1990, The northern margin of the Capricorn Orogen, Western Australia — an example of an early Proterozoic collision zone: *Journal of Structural Geology*, v. 12, p. 685–701.
- WATKINS, K. P., 1983, Petrogenesis of Dalradian albite porphyroblast schists: *Journal of the Geological Society of London*, v. 140, p. 601–618.
- WHITFIELD, G. B., 1987, Wilgeena gold mine, progress report M52/111 and M52/112: Western Australia Geological Survey, M-Series, Item 5862 (unpublished).
- WINDH, J., 1992, Tectonic evolution and metallogenesis of the early Proterozoic Glengarry Basin, Western Australia: University of Western Australia, PhD thesis (unpublished).
- WOODHEAD, J. D., and HERGT, J. M., 1997, Application of the double spike technique to Pb-isotope geochronology: *Chemical Geology (Isotope Geoscience)*, v. 138, p. 311–321.



